Accelerated Stress Testing Results on Single-Channel and Multichannel Drivers: Final Report

U.S. Department of Energy—Solid-State Lighting Technology Area

February 2019

(This page intentionally left blank)

Accelerated Stress Testing Results on Single-Channel and Multichannel Drivers: Final Report

February 2019

Prepared for

Client Name: U.S. Department of Energy

Through contract with
KeyLogic Systems, Inc.
3168 Collins Ferry Road
Morgantown, WV 26505

Prepared by

RTI Authors: Lynn Davis and Kelley Rountree
RTI International
3040 E. Cornwallis Road
Research Triangle Park, NC 27709

Acknowledgments

Disclaimer

Nomenclature or List of Acronyms

7575	75˚C and 75% relative humidity
8585	85˚C and 85% relative humidity
A	ampere
ac	alternating current
AST	accelerated stress testing
CCR	constant current reduction
CCT	correlated color temperature
dc	direct current
DMX	digital multiplex
DOE	U.S. Department of Energy
DUT	device under test
EMI	electromagnetic interference
ESR	equivalent series resistance
Hz	Hertz or cycles per second
IC	integrated circuit
IEEE	Institute for Electrical and Electronics Engineers
I_f	forward current
IP	ingress protection
IV	current-voltage
LED	light-emitting diode
LLC	inductor-inductor capacitor
mA	current in milliamps
mA_{ac}	ac current in milliamps
mA_{dc}	dc current in milliamps
MOSFET	metal-oxide-semiconductor field-effect transistor
MOV	metal-oxide varistor
PCB	printed circuit board
PF	power factor
PFC	power factor correction
PWM	pulse-width modulation

SMPS	switched-mode power supply
SPD	spectral power distribution
SSL	solid-state lighting
TC	thermocouple
THD	total harmonic distortion
TWL	tunable-white lighting
V	volt
V_{ac}	ac voltage
V_{dc}	dc voltage
V_f	forward voltage
V_{th}	threshold or turn-on voltage
W	power in watts
W_{ac}	ac power in watts
W_{dc}	dc power in watts

Executive Summary

Drivers used to operate light-emitting diode (LED) loads form an integral part of the solid-state lighting (SSL) system. While understanding of LED failure modes such as luminous flux depreciation and chromaticity shifts has increased greatly over the past five years, there is still much uncertainty about general failure modes in SSL drivers due to the almost infinite variety of driver typologies. This report, which is the third in a series of three reports on driver robustness, summarizes overall findings from up to 7,500 hours of accelerated stress testing (AST) on two-stage SSL drivers that could be used to operate troffers and similar fixtures. The earlier reports in this series provided initial AST results for both single-channel and multichannel drivers [1] and an interim update on the performance of multichannel drivers in AST [2].

The primary function of an SSL driver is to efficiently convert the energy in the electrical mains (usually alternating current [ac]) into a form that can operate LED loads. The energy conversion is accomplished through a series of circuits that convert the ac energy in the electrical mains into an intermediate direct current (dc) energy, which is then converted into the appropriate waveform to operate the LEDs. Other electronic circuits are needed to provide electromagnetic interference (EMI) suppression, power factor correction (PFC), and other functions, for the SSL driver to operate efficiently, produce minimal total harmonic distortion (THD), and comply with appropriate regulations. This energy conversion can be accomplished using at least two distinct stages in the driver: Stage 1 converts the ac energy into the intermediate dc energy and provides PFC and EMI suppression; Stage 2 converts the intermediate dc energy into a waveform to drive the LED load efficiently. Often, SSL drivers will use either a boost or flyback circuit to provide the Stage 1 intermediate dc voltage with PFC. The Stage 2 circuit typology is typically a buck circuit. The operation of the Stage 1 and Stage 2 circuits is often controlled by separate integrated circuits (IC). Due to the flexibility of LEDs as a light source, the load may be a single LED primary, which can be operated by a single-channel driver, or two or more LED primaries, which can be operated by two or more channels under independent control signals (i.e., multichannel drivers). Typically, each LED primary will be supplied by a dedicated buck converter in the driver.

The AST results provided in this final report demonstrate that many SSL drivers are highly robust and can operate for significant lengths of time in the high-temperature and high-humidity environment of 75°C and 75% relative humidity (7575). As a result, AST is the primary method used to research driver failure mechanisms and their impact on the reliability of SSL systems and their energy consumption over their useful life. In addition, this research also demonstrates that through measuring and tracking electrical properties of SSL drivers, insights can be gained into the residual useful life of the drivers, long before failure occurs, providing insights into parametric electrical failures.

The most common failure mode found in the devices subjected to 7575 testing was failure of the Stage 1 circuits to provide adequate voltages to operate the LED drive circuits in Stage 2. Often failure of the Stage 1 circuits involved the filter capacitors used in the EMI suppression circuit and for PFC. The degradation of these circuits can be detected in advance of failure by monitoring electronic properties of the driver such as power factor (PF) and inrush current. The 7575 exposure studies demonstrated that the change in these properties was most prevalent at dimming levels of 50% and lower.

The photometric changes in LED loads attached to SSL drivers can also provide useful information on the status of the driver. In particular, the photometric flicker behavior of LEDs is controlled by the LED drive waveform generated by the Stage 2 circuits in the driver. These waveforms can be altered by degradation of the circuit components (e.g., capacitors, metal-oxide semiconductor field-effect transistors [MOSFETs]) in the buck converters that form the heart of Stage 2 or by degradation of the Stage 1 circuits such that inadequate voltages are supplied to operate the Stage 2 electronics. A close examination of the photometric flicker waveform produced by the SSL driver provides a monitor of the relative extent of these two potential failure modes, long before complete failure of the driver occurs.

In these tests, some single-channel and multichannel drivers are still operating near full capabilities after 6,000 hours and 7,500 hours, respectively, in the 7575 environment. All of the samples studied in these test conditions survived for at least 1,000 hours, demonstrating the generally robust performance of SSL drivers. This research also demonstrated that certain electrical properties (e.g., power factor, inrush current, photometric flicker waveform) could be monitored to provide insights into the degradation of SSL driver electronics, before device failure occurred. This information is useful not only for predicting the health of SSL driver, but in future research aimed at reducing the impact of electronics failure on SSL device reliability.

Table of Contents

List of Figures

List of Tables

1 Introduction

1.1 Drivers for LED Operation

1.1.1 LED Properties

A light-emitting diode (LED) is a non-linear semiconductor device with an impedance that is related to the voltage applied across its terminals. This characteristic of LEDs produces the well-known hockey-stick shape of the current-voltage (IV) profile that is shown in **Figure 1-1**. When forward biased, the impedance of a LED is proportional to the inverse of the slope of the IV curve, the impedance is essentially infinite below a turn-on or threshold voltage (V_{th}) and a low value above V_{th}. The value of V_{th} for a LED depends on several factors including the semiconductor chemistry, doping, and the operational temperature [3].
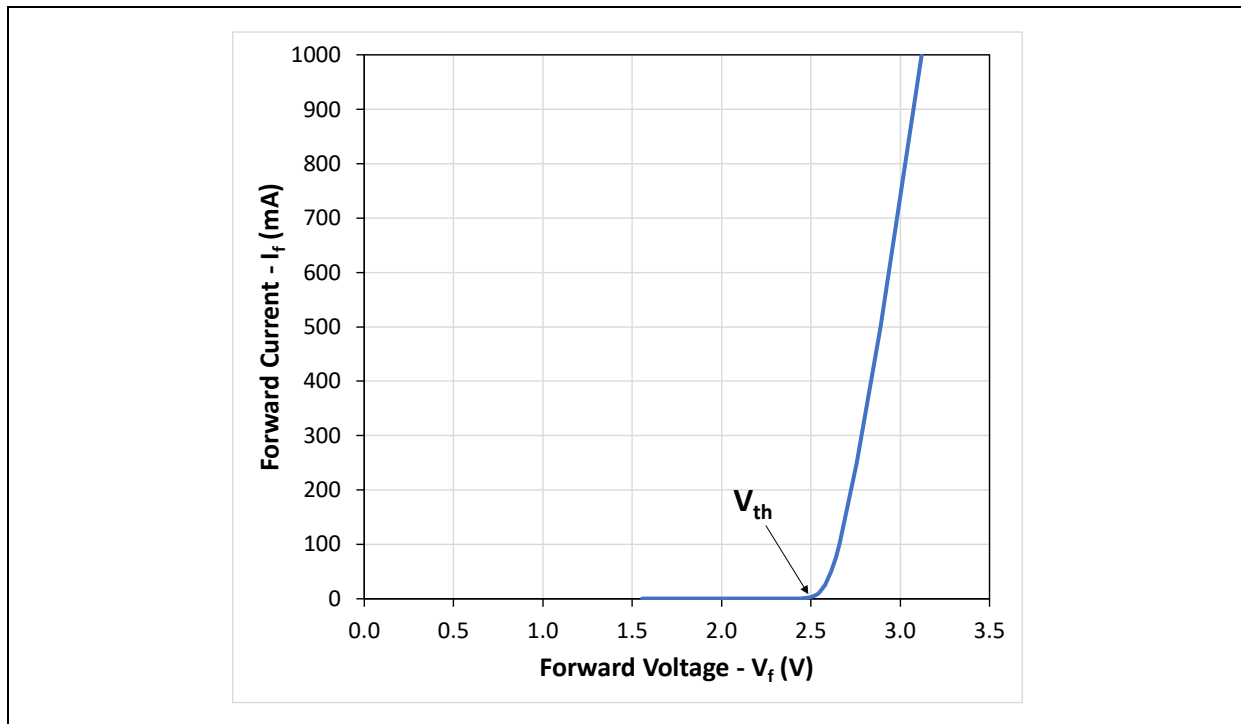
Figure 1-1. Representative IV curve of a LED.

The intrinsic characteristics of LEDs shown in Figure 1-1 indicate that the forward voltage (V_f) applied to the LED determines the forward current (I_f), which, in turn, is proportional to the light output. The impedance of a LED is very low above V_{th}, so a current-limiting resistor is usually placed in series with each LED string to control the maximum amount of current that can pass. Otherwise, excessive current could flow through the circuit damaging the LED. Since the intensity of light produced by a LED is determined by I_f, it is important for I_f to remain constant. However, as LEDs operate and produce heat, the temperature of the LEDs increase, causing V_f to decrease. To compensate for changes in V_f with temperature, virtually all LED drivers provide a tightly controlled constant current and adjust the voltage output waveform to produce a consistent light emission.

Dimming or adjusting the light output from a LED can be achieved in several ways as shown in **Figure 1-2**. The most straightforward method is to provide an appropriate forward current (I_f) (as a direct current [dc] waveform) and to adjust LED brightness by changing the supplied I_f value (see Figure 1-2A). This method is commonly referred to as constant current reduction (CCR), which is often achieved with a linear power supply. The primary advantages of the CCR approach are that it produces minimal to no photometric flicker and there are no electromagnetic interference (EMI) issues. However, these power supplies may have reduced

efficiencies due to increased electrical dissipation. Another approach to adjusting the brightness of LEDs is to turn the LEDs on and off with some duty cycle so that the integrated LED intensity sensed by the human eye achieves a value that is less than that of the LEDs if continuously operated. Switching of the LEDs is usually achieved with a switched-mode power supply (SMPS). Through judicious control of the duty cycle (i.e., the time the LED is turned on divided by the total on-time and off-time for the LED), accurate LED intensity control can be achieved. This approach, which is termed pulsed-width modulation (PWM), can improve the energy efficiency of the driver supplying the LED but can also create the sensation of photometric flicker and produce EMI [4]. An example of a PWM waveform is shown in Figure 1-2C. Without adequate precautions, PWM signals can produce large amounts of photometric flicker in LEDs that are visible to the eye unless the modulation frequency is very high [e.g., greater than 3,000 Hertz (Hz)] or the modulation range (i.e., the difference between the maximum and minimum modulation values) is low. A third method to adjust the light output from a LED is to create a hybrid waveform of the PWM and CCR signals as shown in Figure 1-2B. The hybrid waveform consists of a dc baseline value to which a PWM modulation signal is applied. If the dc component of the hybrid waveform is below V_{th}, the LEDs will only turn on when the superimposed PWM modulation drives V_f to a value above V_{th}. In many instances, a consistent flicker frequency occurs in both the PWM and hybrid modulation schemes, although there are some designs in which the flicker frequency and modulation range can vary as well to produce higher efficiencies.
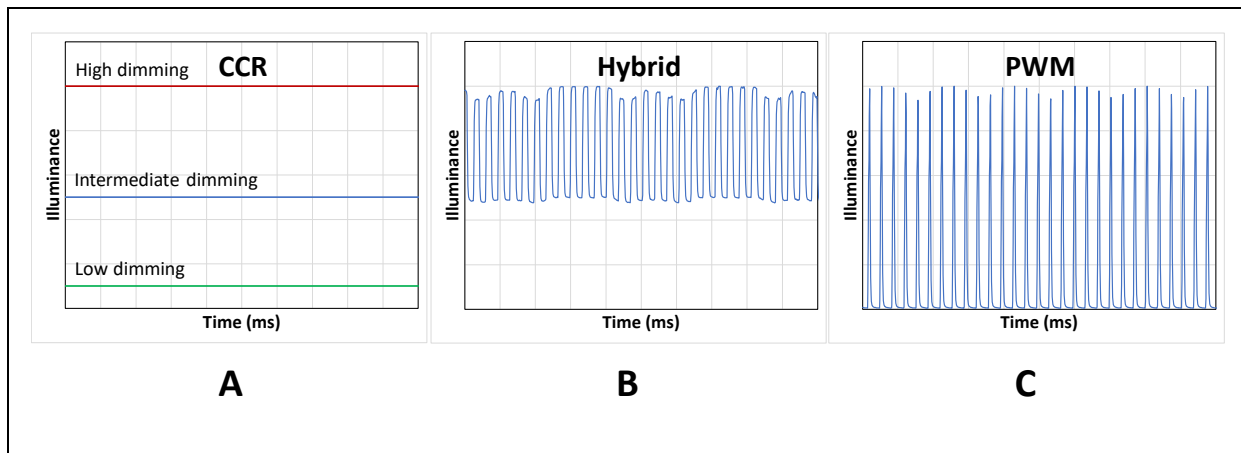
Figure 1-2. Methods used to dim a LED.

Many LEDs used in solid-state lighting (SSL) sources have a fixed emission spectrum and can be operated with a single dc output from the driver. Such lighting sources normally utilize only one LED primary, which can be configured as a group of LEDs connected in series and/or parallel. All LEDs in this LED primary have similar emission characteristics (e.g., spectral power distribution [SPD], luminous flux), and each LED primary can be either a white emitter (e.g., warm white, cool white) or a color emitter (e.g., red, green, blue) [5].

The ease with which multiple LED primaries can be incorporated into an SSL light source has opened the possibility of new lighting products with dynamic lighting properties. For example, multiple LED primaries can be combined into a single SSL device to create tunable-white lighting (TWL) fixtures [5, 6], which have many applications, including lighting in educational settings [6–9], senior centers [10], and healthcare facilities [11]. A typical example of a TWL device comprises both warm white and cool white LEDs. In this system, the two sets of LED primaries provide the end points of the tuning range. The combined emission spectra from the LED primaries can be adjusted in a linear fashion between the two end points by changing the current to each LED primary through separate driver channels creating different light spectra and correlated color temperature (CCT) values [2, 5].

1.1.2 Overview of Driver Structure

Drivers used to power SSL lamps and luminaires are complicated devices comprising multiple electrical circuits, each designed for a specific purpose. The intent of this collection of electrical circuits is to efficiently convert energy from the electrical mains into a form that can operate LED loads. The basics of driver construction have been reviewed previously [1, 2] and will only be summarized here. In general, SSL drivers accomplish the conversion of electrical energy in the mains to light emission energy through several steps: (1) converting the energy in the ac mains to an intermediate dc energy; (2) providing power factor correction (PFC) of the load to the ac mains; and (3) converting the intermediate dc energy to an appropriate electrical output waveform to drive the LEDs. As mentioned in Section 1.1.1, this electrical output energy waveform can be either a CCR, PWM, or hybrid signal.

SSL drivers are designed to maximize the efficiency of converting the ac energy in the electrical mains to the appropriate waveform to drive the LEDs while minimizing total harmonic distortion (THD), EMI emissions, and photometric flicker. The most common driver architecture is the SMPS, and the primary source of inefficiency for SMPS devices is switching losses associated with turning the metal-oxide semiconducting field-effect transistor (MOSFET) on and off [12, 13]. Fortunately, these inefficiencies can usually be minimized by proper design and component selection, and the SMPS driver can be highly efficient. However, the SMPS driver can also produce EMI, due to the switching, so EMI suppression circuits are typically added to limit the level of conductive emissions that are injected back onto the ac mains [14]. EMI filters, consisting of series and parallel combinations of capacitors and inductors are placed after the metal-oxide varistor (MOV) [15]. The output of EMI filters are fed to the electronics, so changes in this voltage could affect system operation. Another common driver supply typology is the linear power supply, which is simple to build but is generally less efficient than SMPS devices due to higher levels of electrical energy dissipation [12]. Age-related degradation of the components in driver circuits, especially those directly involved in providing power, can cause the performance of the SSL device to fall outside of end-users' expectations, possibly to the point of being classified as a failed device. For example, THD and photometric flicker are primarily impacted by the PFC and LED drive circuits, respectively, and their performance can change significantly as components age. However, monitoring the behavior of these circuits may provide insights into the health of the driver, long before failure occurs.

Depending on the space requirements and performance specifications of the SSL driver, the PFC and dc–dc conversion stages can be optimized together or separately. Combining the function of the two circuits and optimizing their joint performance provides a single-stage driver. The advantage of this approach is that the overall driver size and parts count can often be reduced, making single-stage drivers ideal for lamps and other small SSL devices. If the performance of the PFC and LED drive circuits are optimized separately, a two-stage driver with two power conversion stages (i.e., ac/intermediate dc and intermediate dc/output waveform) is produced. In many two-stage designs, a boost or flyback circuit is used in the PFC stage to produce an intermediate dc voltage with high PF and low THD, while a buck circuit is used to produce the final waveform to drive the LEDs [1, 2, 12, 13].

1.2 SSL Driver Configurations and Common Use

SMPS driver configurations vary with the LED lighting application and are intended to maximize device efficiency, minimize cost, and provide sufficient control to meet a specific lighting application. Due to their widespread use in troffers and outdoor luminaires, this report will focus on two-stage drivers—those utilizing at least two separate power conversion stages to create the output LED waveform. In addition to the number of power stages, an SSL driver can be further classified as being single-channel (if it has only one output channel to drive a single LED primary) or multichannel (if it has two or more output channels to independently drive two or more LED primaries). A schematic of a two-stage, single-channel driver is shown in **Figure 1-3**. In this driver structure, the power in the input ac mains passes through a rectifier to convert it to dc. This process and the PFC and THD control functions are generally accomplished using either a flyback or boost converter that is controlled by Control IC 1. Outputs from this first stage and a control signal (e.g., typically a setting for

dimming level) are supplied to Control IC 2 to generate the appropriate electrical waveform for the stand-alone LED primary. Figure 1-3 presents a generalized schematic of a two-stage single-channel driver; additional components (e.g., capacitors, inductors, resistors, MOSFETs) associated with potential driver typologies and other circuits (e.g., EMI suppression, PFC) are omitted for convenience.
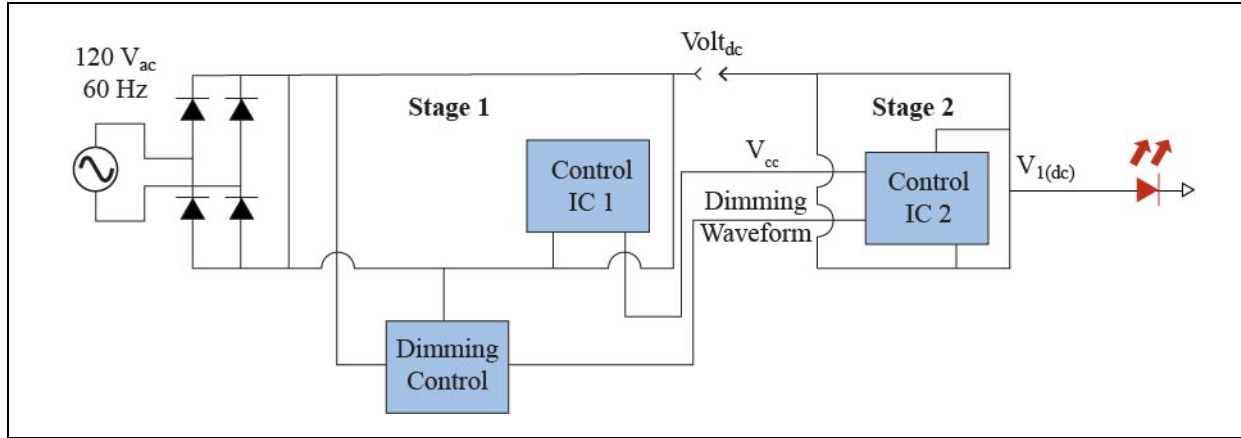
Figure 1-3. Schematic of a two-stage, single-channel driver.

Drivers with independent output channels for each LED primary can be classified as multichannel drivers. As with a single-channel driver, the first stage in a multichannel driver converts the ac energy from the electrical mains into an intermediate dc waveform that is fed to Control IC 2. A control signal containing information on both lighting color and dimming levels is also simultaneously fed to Control IC 2. **Figure 1-4** presents a generalized schematic of a two-stage multichannel driver; additional components (e.g., capacitors, inductors, resistors, MOSFETs) associated with potential driver typologies and other circuits (e.g., EMI suppression, PFC) are omitted for convenience.
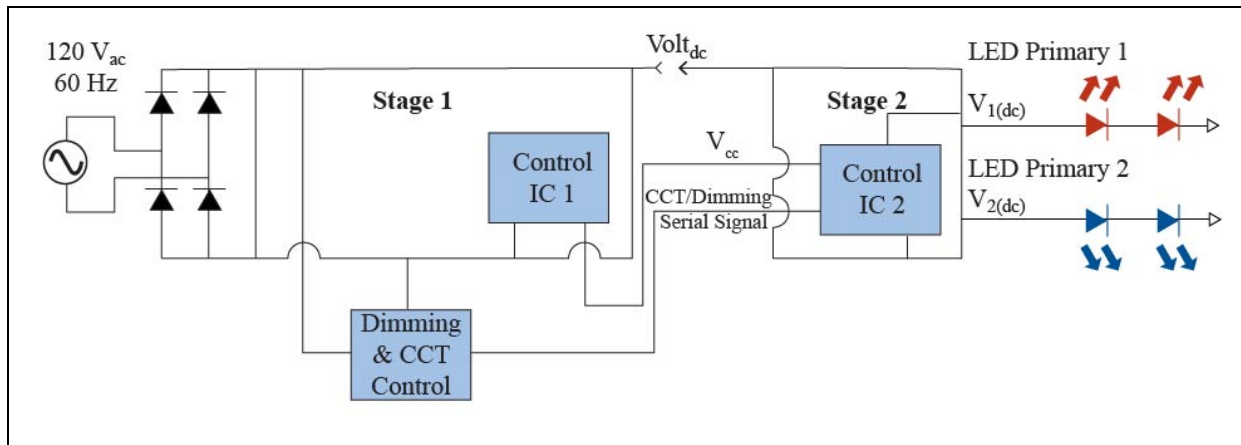
Figure 1-4. Schematic of a two-stage dual-channel driver for operating a TWL system with two LED primaries.

The controllability of the multistage driver is built primarily into the second stage. Often, the circuit typology of Stage 2 is a buck converter, which is a relatively simple circuit consisting of a MOSFET switch, an inductor, a capacitor, and a diode configured as shown in **Figure 1-5**. The waveforms shown in Figure 1-2 are generated by opening and closing the MOSFET switch in the buck circuit with the capacitor providing power and the diode controlling current flow when the switch is open. Each output channel in a multichannel driver has a dedicated buck circuit.
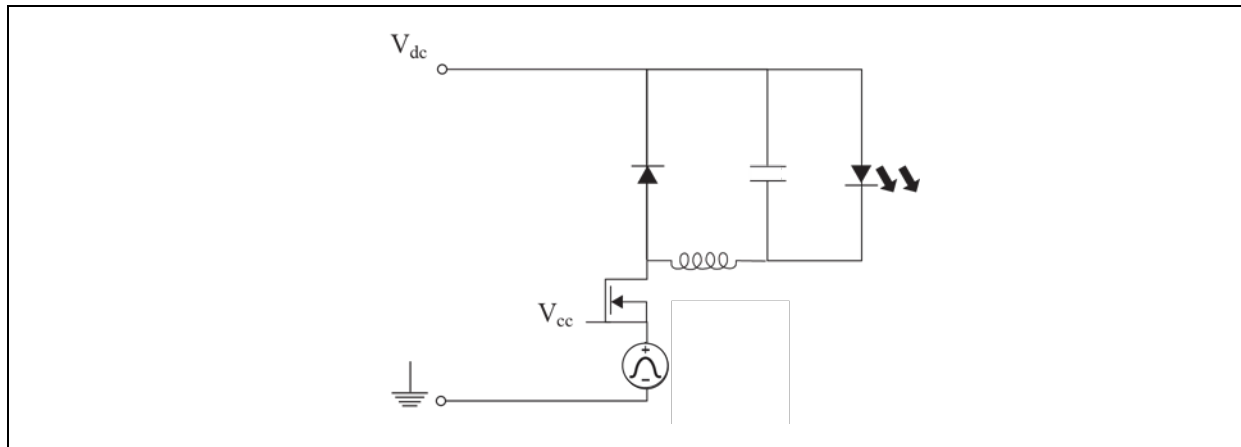
Figure 1-5. Detailed schematic of the buck converter often used as the LED drive circuit to control the power delivered to the LEDs in a multistage driver.

During operation, the logic circuits in Control IC 2 translate the dimming and CCT control signal to generate waveforms for the LED primaries, with each waveform operating a LED primary in a manner where the combined output of all LED primaries produces light at the CCT and dimming level specified by the control. When the control signal enters Control IC 2, a series of logic gates and other components individually adjusts the duty cycles of the MOSFETs in the different buck channels and each channel can have a different duty cycle. A duty cycle close to 1 is equivalent to a near-constant on-state for the LED and applies a minimal reduction to the average power delivered to the LED primary (from the intermediate dc power supplied by Stage 1). In contrast, a duty cycle close to 0 is equivalent to a near-constant off-state for the LED and applies a large reduction to the average power delivered to the LED primary. Through these adjustments, the necessary power is supplied to each LED primary circuit to obtain the light output. In addition, the heat generated by the MOSFET in the buck circuit will depend on both the current flowing through the circuit and the switching frequency [16]. If this heat is not adequately transferred to the case, other components near the MOSFET could heat up as well, which will impact their reliability. For example, the reliability of film capacitors is known to be strongly influenced by temperature [17].

In many devices, the output waveform is delivered through a buck circuit (see Figure 1-5), and any degradation in these circuit components, especially the capacitor, could alter the waveform delivered to the LED, which can impact the properties of emitted light including intensity, CCT, and flicker. Low dimming levels are especially sensitive to changes in the capacitor in the buck circuit, and these changes can be manifested as alterations of the flicker waveform or a change in the decay constant of a PWM pulse [1, 2]. In addition, the performance of the circuits in Stage 1 of the driver can impact flicker if the degradation of these circuits leads to inadequate voltages being supplied to the Stage 2 circuitry. As a result, the change in the photometric flicker properties of an SSL source may provide insights into the health of the SSL driver, even in a fully functional unit.

1.3 Common SSL Driver Failure Modes

Depending on their design, specification, and operational environment, all electrical components used in SSL drivers are subject to failure during the course of operation. Electrical failure is often precipitated by environmental stresses such as heat, humidity, electrical voltages, electrical transients, changes in power quality, and other factors. A list of potential failure modes of components in SSL drivers is given in **Table 1-1.** The most common failure sites in SSL devices are the capacitors and MOSFETs [13, 18, 19, 20].

In addition to component failures, fracture of the solder joints connecting the driver components to the printed circuit board (PCB) is another possible failure mode. In well-controlled soldering processes, solder joint fatigue caused by the growth of brittle intermetallics is the root cause of wear-out failures that provide an

upper limit to device life [21]. Unfortunately, poorly controlled soldering processes can produce low solder joint quality resulting in latent defects such as inadequate solder wetting or cold soldering that result in premature failure [22]. Such failure modes are not considered in this analysis.

Table 1-1. Failure modes and environmental stressors for SSL driver components.

Component	General Use in SSL Drivers	Common Failure Mode	Environmental Stressors	Reference
Electrolytic capacitor	EMI filters Energy storage for LED output waveform	Electrolyte loss through leakage or degradation Increases in equivalent series resistance (ESR) Drop in capacitance	Temperature Electrical voltage Electrical signal quality, especially transients	18, 19, 20
Film capacitor	EMI filters Energy storage on LED output waveform	Lead corrosion Drop in capacitance through "self-healing" effect	Humidity Electrical voltage Electrical signal quality, especially transients Temperature	17, 18, 20
MOSFETs	Switching modulation of LED primaries Switching operation of Stage 1 flyback converters	Shorting between the collector and emitter terminals due to dielectric breakdown, hot carrier injection, or excessive temperature from poor heat sinking	Temperature Current level and electrical signal quality, especially transients	18, 20
MOV	Surge protection and suppression	If the surge suppression rating is exceeded, the component may become a short and stop providing protection	Electrical signal quality, especially number and intensity of transients	23
Resistors and diodes	Setting and controlling current levels	Excess current can create an open circuit component for resistors or a short for diodes	Current level and electrical signal quality, especially transients Temperature	18, 20

2 Experimental Procedures

2.1 Accelerated Stress Tests

Accelerated stress testing (AST) is the recommended approach to study design flaws, manufacturing defects, and overall robustness of LED products [19]. The results reported here are a continuation of previously reported testing regiments, so the same testing procedures will be used. Specifically, the stand-alone drivers examined in this study were subjected to AST at nominal conditions of 75°C and 75% relative humidity (7575). There are several reasons why this ambient testing environment was chosen. First, as demonstrated in Table 1-1, the application of heat/humidity generally shortens the lifetime of the electrical components in SSL devices. Further, the 7575 test was chosen because previous studies demonstrated that this environment provided reasonable acceleration for integrated SSL drivers used in 6" downlights [20]. Finally, the 7575 method was chosen because more aggressive conditions such as 85°C and 85% relative humidity (8585) can distort certain plastics and trigger thermally induced reduction in the operation of some driver electronics.

The details of the 7575 AST procedure used in this testing are provided elsewhere [1, 2], and are only summarized here. During 7575 testing, the devices under test (DUTs) were placed inside an environmental chamber that was capable of controlling temperature and humidity. The DUTs were connected to external LED loads using high-temperature silicone-coated wires that passed through openings in the chamber walls. This testing setup allowed only the drivers to be exposed to the 7575 environment while maintaining the LED primaries in a room temperature environment. Consequently, only the drivers were stressed by the AST conditions, isolating any effects attributable to the aging of the driver from those caused by changes in the load.

The testing protocol required that the DUTs undergo power cycling with a 50% duty cycle with a period of two hours (i.e., one hour on and one hour off) while in the 7575 environment. Environmental exposure of the DUTs was typically performed in increments of either 250 or 500 hours, and the degradation of the DUTs was monitored during the 7575 exposure and at the end of each exposure increment. The temperature rise of the DUTs during power cycling was continuously measured during the 7575 exposure using Type-K thermocouples (TC) placed near the transformer in the Stage 1 flyback circuit and the switching MOSFETs in Stage 2, as described in previous reports [1, 2]. TC readings were taken every 10 minutes using a data-logging program running on a computer.

2.2 Measurement Methods

2.2.1 Electrical

The electrical characteristics of the DUTs examined in this study were measured at various stages of the 7575 exposure using a Xitron 2802 two-channel power analyzer. An unexposed driver of the same product was used as a control and measured concurrently. In obtaining the power characteristics, the driver and LED loads were configured as for the 7575 experiments except that external connections were made to the power analyzer to measure (1) the input ac mains power and (2) the output dc power supplied by the driver to each channel. A power analyzer provides more capability than a simple meter including the ability to measure both the ac and dc electrical properties of an electrical waveform as a voltage (measured in volts [V]) and current (measured in amperes [A] and milliamperes [mA]). The power analyzer test was also used to determine other electrical properties such as THD and the total inrush current for both the control and 7575 sample. The power analyzer computes inrush current by recording the current data for the first 63 milliseconds of operation, converting this signal to the Fourier space, and taking the highest value as the inrush current. Some drivers were also tested for performance under dimming conditions, and either a LED-compatible 0-10 volt dimmer (Lutron Diva) or a digital multiplex (DMX) control head (Finetune User Interface by Finelite Inc.) were used to set dimming levels.

2.2.2   Photometric

Because the LED loads were placed on top of the test chambers, the photometric flicker properties could be readily measured at any time during 7575 exposure. Flicker measurements were only taken after the drivers had cooled to 25˚C before being turned on to eliminate any effects from heat provided by the environmental chamber. To monitor any change in the flicker characteristics of the LED loads attached to a DUT, a handheld spectral flicker meter (GigaHertz-Optik BTS256-EF), operating under computer control, was used in conjunction with an integrating sphere. The properties of this flicker meter and experimental setup have been discussed previously [1, 2, 24]. This configuration allowed a number of photometric properties to be measured for each sample (e.g., % flicker, flicker frequency, SPD) with minimal interference from other samples and overhead lights.

In addition to measuring the photometric flicker properties of the LED loads, the electrical waveforms delivered from the driver to each LED primary were measured using a Fluke 124 ScopeMeter attached to a computer. These measurements allowed a determination of the exact waveform (i.e., pulse width, pulse amplitude, and period) driving the operation of each LED primary. This information is complementary to the flicker signal, since the measured photometric flicker is an aggregate of the light output from all the LED primaries whereas the electrical signals provided to each primary could be studied with the ScopeMeter. Deconvoluting the waveforms used for each individual LED primary is easier to do electrically than photometrically, due to the faster response time of the ScopeMeter.

3 Findings

3.1 Single-Channel Drivers

Three different single-channel driver products (designated DUT-S1, DUT-S2, and DUT-S3) were exposed to the 7575 environment for up to 6,000 hours. The drivers were contained in an environmental chamber and attached to an external LED load that was placed outside the environmental chambers (see Section 2.1). The LED loads were chosen such that they required 95% of the maximum specified current for each driver. Two samples of each DUT were examined during this test to replicate the results. As there are a and b samples for each DUT, the individual samples are designated as DUT-S1a, DUT-S1b, and so forth. All three DUTs were Class 2 drivers that can operate at input ac voltages between 120 V and 277 V, although all devices were operated at 120 V during these tests. In addition, all three products were rated for surge protection of 2.5 kV (per IEEE C62.41), equipped with 0–10 V dimming capability, and qualified for the Underwriter's Laboratory damp and dry environmental protection rating. The interiors of DUT-S1 and DUT-S3 were encapsulated with a hard, black epoxy intended to provide environmental protection and promote heat dissipation. The interior of S2 was not encapsulated but there were thermally conductive pads on the power diodes and MOSFETs to transfer heat to the case. Additional specifications for these products are given in **Table 3-1**.

Table 3-1. Manufacturer's specifications for the single-channel drivers examined in this study.

Driver No.	Output Voltage Range (V)	Output Current Range (mA)	Max Output Power (W)	Driver Efficiency	PF	THD @ Max Load	Max Case Temp °C
DUT-S1	10–55	400–1,400	50	85%	>0.9	<10%	75
DUT-S2	27–54	100–1,100	40	85%	>0.95	<10%	75
DUT-S3	15–53	11–1,050	55	88%	>0.95	<20%	85

[1] The values in the table are given for 120 V operation only.

The functional status for each single-channel driver sample subjected to the 7575 environment is given in **Figure 3-1**. The cumulative operational time of each sample is indicated by the length of the horizontal line with a red line denoting a sample that ultimately failed and a green line denoting a sample that is still operating after 6,000 hours of 7575 exposure.[1] For failed samples, the location of the red X in Figure 3-1 denotes the failure time as determined by a change in sample temperature recorded by the TC attached to each device. In some instances, a partial failure was evidenced by a small temperature reduction when the sample was operating, as shown in **Figure 3-2** due to a drop in the electrical energy being dissipated by the device. Ultimately, the temperature of any completely failed device will remain near the ambient temperature during testing (also shown in Figure 3-2). As indicated in Figure 3-1, both DUT-S2 samples were still operational after 6,000 hours of testing, whereas both samples of DUT-S1 and DUT-S3 failed in less than 4,800 hours.

Using these data, a two-parameter Weibull plot was created for the single-channel drivers and is shown in **Figure 3-3**. In this analysis, the exact failure time (as noted from the TC readings) was used and the end time of the last experiment (6,000 hours) was used for the suspended samples (i.e., DUT-S2a and DUT-S2b). From the Weibull analysis, the shape parameter (a.k.a., the Weibull slope, which is denoted as β) was calculated to be 2.92, and the Weibull scale parameter (a.k.a., the Weibull characteristics life, which is denoted as η) was calculated to be 5,480 hours. Because the scale parameter is greater than 1, the failure rate is accelerating with time, which is consistent with 7575 being an accelerating test.

---

[1] NOTE: The operational times have not been corrected for the 50% duty cycle (i.e., 1 hour on and 1 hour off) that was used in this testing.
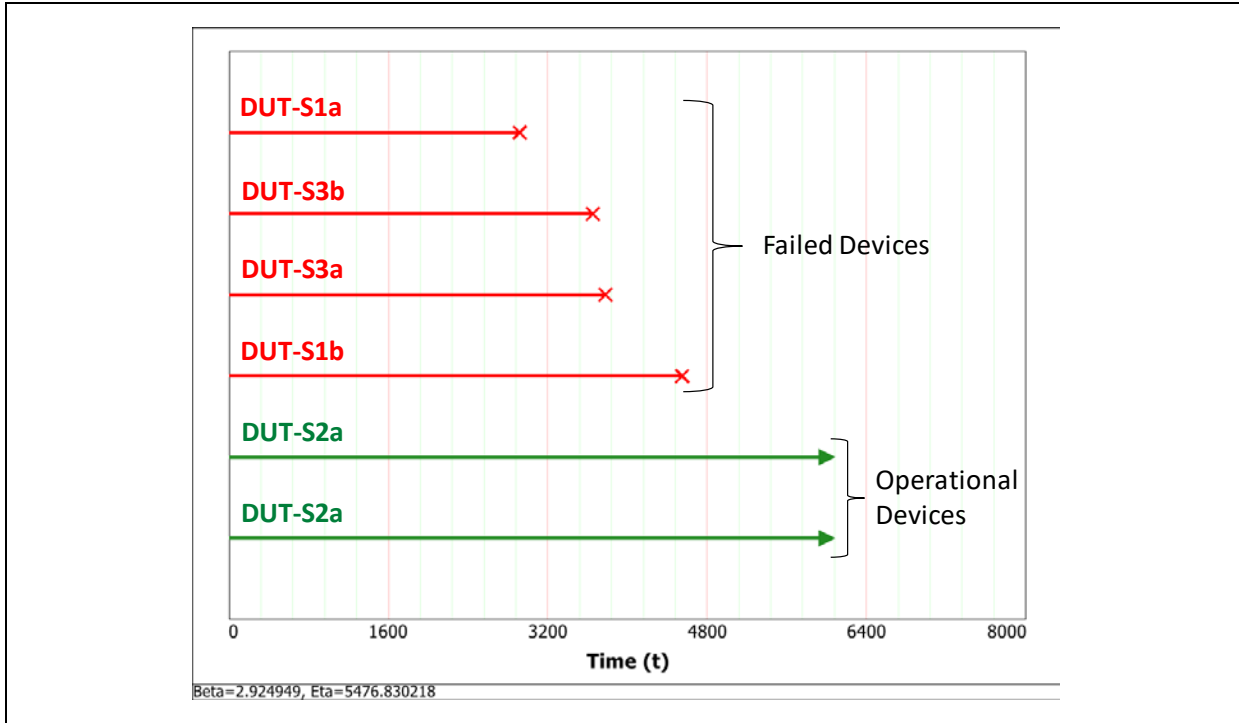
Figure 3-1. Functional status (red = failure, green = operational) and operational time of single-channel drivers during 7575 testing.
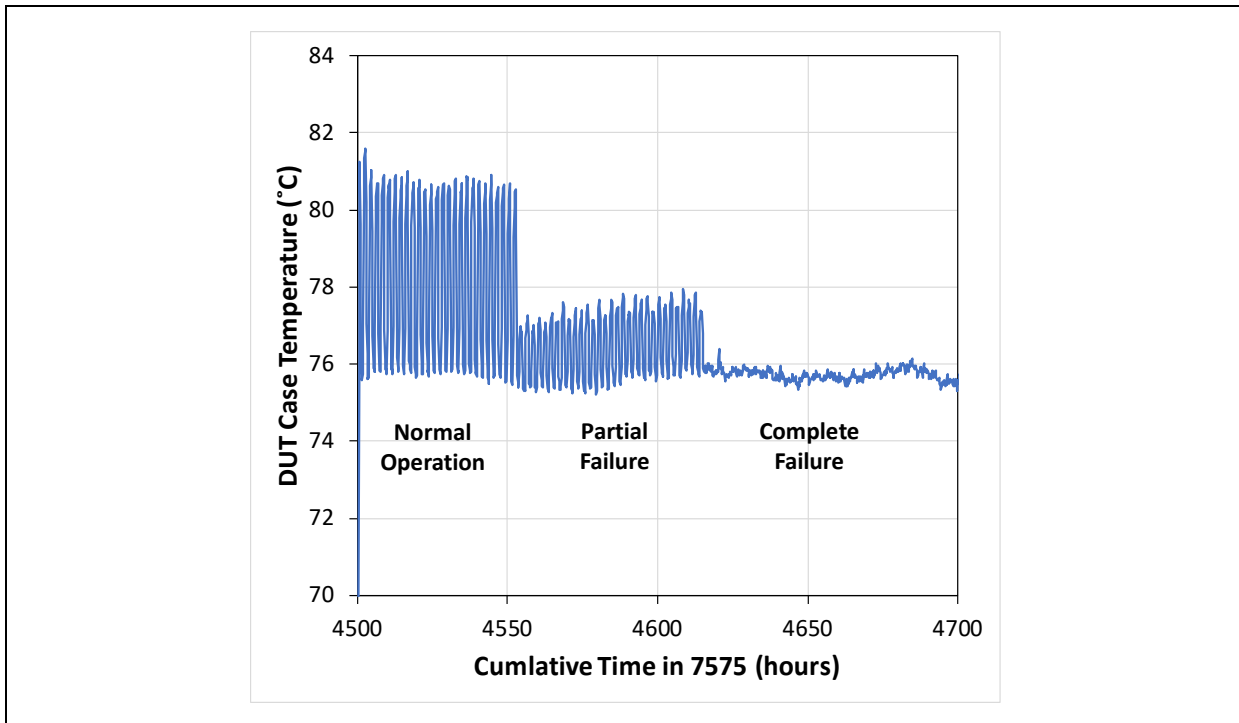

Figure 3-2. Temperature profile of DUT-S1b during 7575 testing.
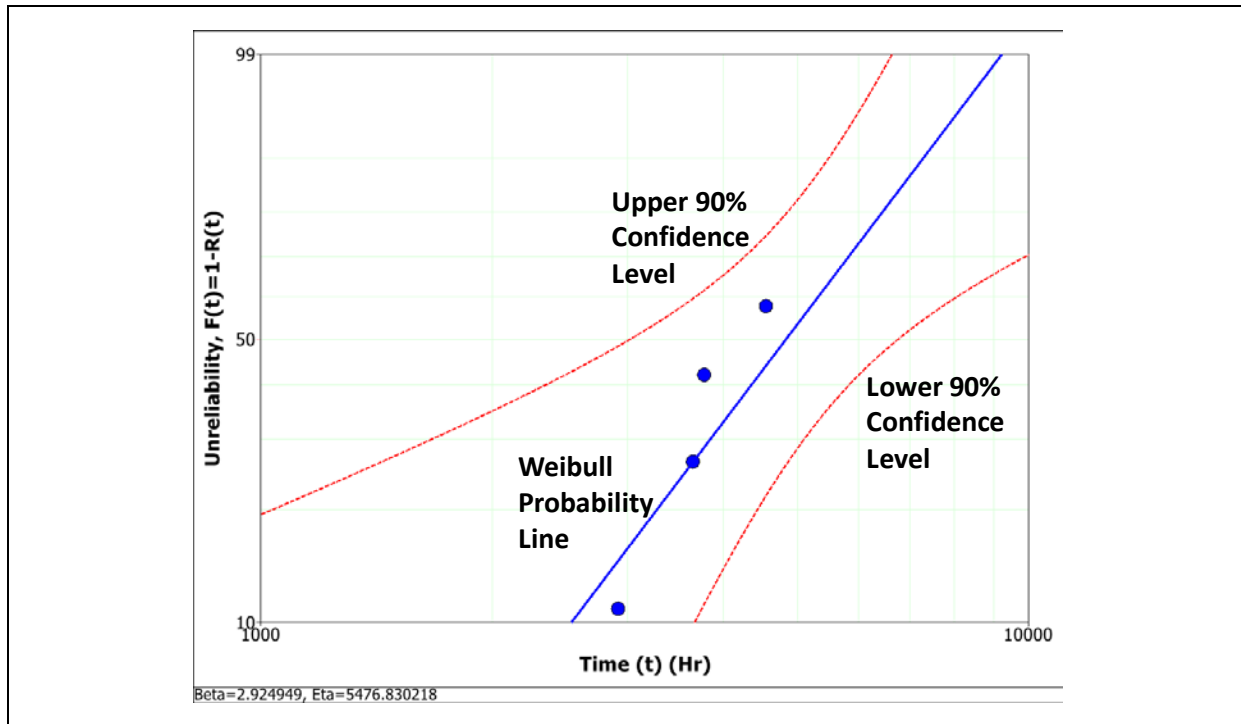
Figure 3-3. Two-parameter Weibull plot for the single-channel drivers operating in the 7575 environment.

Additional details on test results for DUT-S1, DUT-S2, and DUT-S3 are given below. In the case of DUT-S2, the devices were fully operational at the end of testing and could be subjected to full electrical and photometric testing. For the other devices, either no testing was possible (e.g., a complete failure occurred) or only rudimentary electrical testing could be performed due to intermittent behavior. In the case of DUT-S3b, the sample exhibited excessive flicker above 3,658 hours of operation in the 7575 environment and was classified as a failure. However, a limited battery of electrical and photometric testing could still be performed on this sample.

3.1.1 DUT-S1

The driver typology for DUT-S1 consists of a flyback circuit in Stage 1 followed by a buck circuit in Stage 2. This device accomplishes light dimming using a hybrid waveform with a predominantly dc waveform, with a small ripple (flicker % = 0.7% and flicker frequency = 1,940 Hz) at high light output and a full PWM dimming signal at low levels (flicker % = 100% and flicker frequency = 1,940 Hz. Both DUT-S1a and DUT-S1b failed in a similar manner although at different times (see Figure 3-1). Neither sample produced light from their LED loads after failure occurred, and their power consumption dropped significantly. However, both samples still consumed power but at a lower level than specified after failure (see Table 3-1), and only rudimentary electrical tests could be performed on these devices. As shown in **Table 3-2**, there was a reduced inrush peak current of 1,730 mA, compared to a value of 2,470 mA for the control, and the operational current dropped from 1,060 mA in the control to 3.26 mA for the failed device. The PF value of the failed devices was also significantly different from that measured for the control. All of these factors (e.g., lower inrush current, reduced PF) point to failure occurring in the Stage 1 circuit. The ultimate source of failure could not be fully identified because the device is potted, but an arcing noise and strong smell originated from the flyback transformer and switching MOSFET pair in the flyback circuit in Stage 1, suggesting that this site is the failure location for both samples.

Table 3-2. Electrical properties of DUT-S1b after failure in the 7575 test.

Dimming Signal (V)	Total Input Voltage (V$_{ac}$ & V$_{dc}$)	Inrush Peak Current (mA$_{ac}$ & mA$_{dc}$)	Total Input Current (mA$_{ac}$ & mA$_{dc}$)	Output Voltage (V$_{dc}$)	Output Current (mA$_{dc}$)	PF	Volts %THD
10.04	121.00	1,730	3.26	1.06	0.00928	0.40	3.86
5.09	121.00	1,730	3.24	0.92	0.0167	0.42	3.88
1.35	121.00	1,730	3.22	1.21	0.00731	0.42	3.86

3.1.2   DUT-S2

DUT-S2 is a linear driver that accomplishes light dimming using a CCR waveform, so only the dc current level supplied to the LED changes with dimming. There are no modulating waveforms as with DUT-S1. The % flicker produced by the control device was very low, typically 0.3% or less at all dimming control voltages. The photometric response at different dimming levels for the DUT-S2a sample after 6,000 hours of exposure to 7575 is shown in **Figure 3-4**. Similar behavior was observed for DUT-S2b. For both samples, the measured flicker percentage was below 0.5% at all dimming control settings, which is consistent with a dimming control based on CCR. There was no significant difference between the performance of the control and the post-7575 samples, indicating that the overall change in the electrical circuit was minimal through 6,000 hours of 7575 exposure.
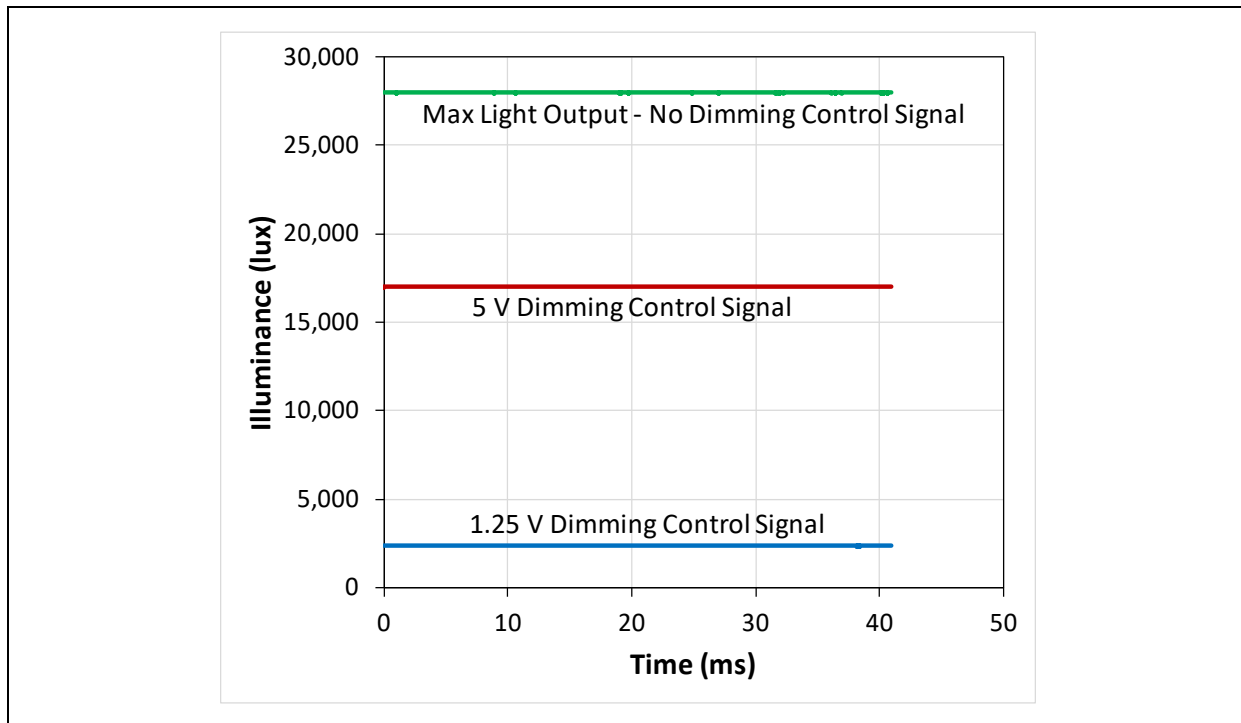
Figure 3-4. Photometric response of DUT-S2a after 6,000 hours of operation in the 7575 environment.

Both DUT-S2a and DUT-S2b were fully operational at the end of 6,000 hours in the 7575 environment. The level of degradation observed for these samples was minimal, and their electrical properties at different levels of dimming are shown in **Table 3-3**. The dimming behaviors of the control and the 7575 exposed samples were also similar as shown in **Figure 3-5**, further indicating minimal change as a result of 7575 exposure.

Table 3-3. Average electrical properties of DUT-S2a and DUT-S2b after 6,000 hours of operation in 7575.

Dimming Signal (V)	Total Input Voltage (Vac & Vdc)	Inrush Peak Current (mAac & mAdc)	Total Input Current (mAac & mAdc)	Output Voltage (Vdc)	Output Current (mAdc)	PF	Volts %THD
9.38	121	10,600	368	43.4	873	1.00	3.91
5.01	121	19,500	215	42.0	519	1.00	3.89
1.25	121	10,500	42.0	39.0	69	0.97	3.87

Figure 3-5. The driver output power, as a function of dimming control voltage, for the DUT-S2 control and samples DUT-S2a and DUT-S2b after exposure to 6,000 hours of testing in the 7575 environment.

A detailed analysis of the electrical data found some evidence of a low amount of degradation in the electrical components of both DUT-S2 samples subjected to 7575 exposure. Most notably, the PF values of both samples were higher (at dimming control signals of 4 V or less) for the two samples exposed to 7575 compared to the control (see **Figure 3-6**). This finding is consistent with the driver exhibiting increased resistance and a reduction in capacitance as 7575 exposure increases. We also observed a reduction in the inrush current into the driver, as shown in **Figure 3-7**, which is also consistent with an increased resistance and lower capacitance in the circuit. We have previously demonstrated that this behavior can indicate the degradation of the EMI filter capacitors in the PFC circuit [2]. As the capacitance in the EMI filter drops, the resistance increases and the load takes on more linear characteristics.

Figure 3-6. PF, as a function of dimming control voltage, for the DUT-S2 control and samples DUT-S2a and DUT-S2b after exposure to 6,000 hours of testing in the 7575 environment.
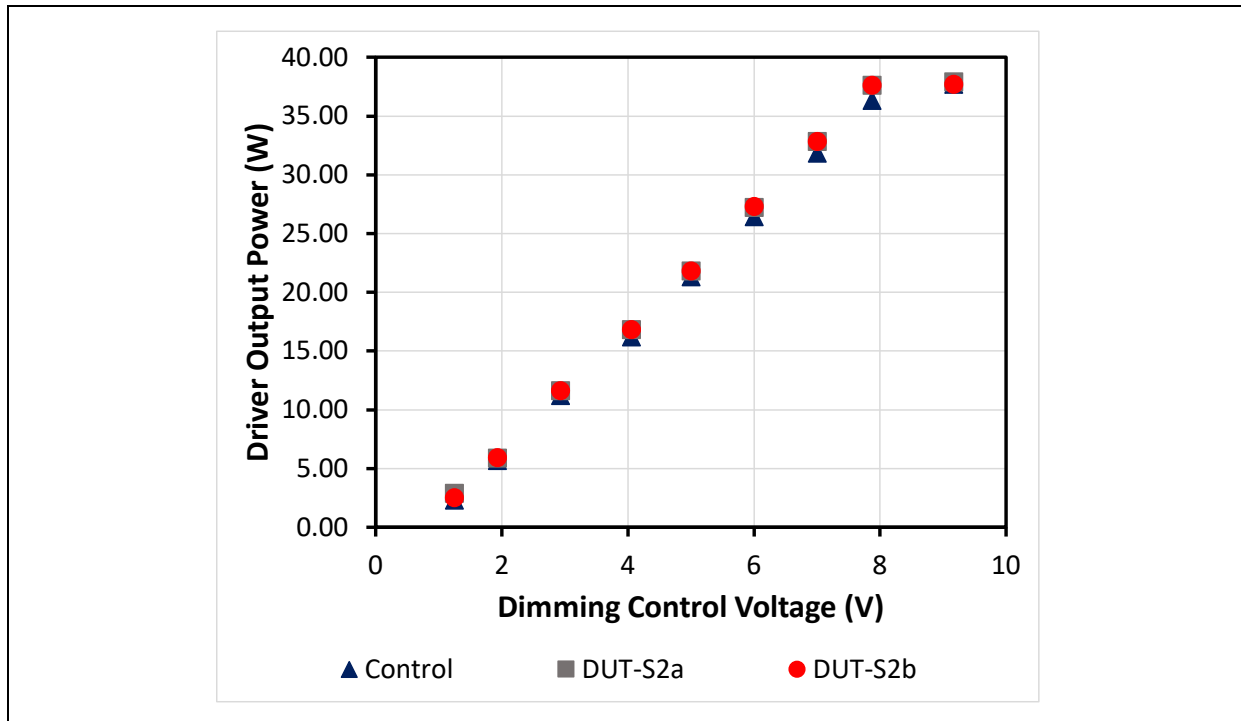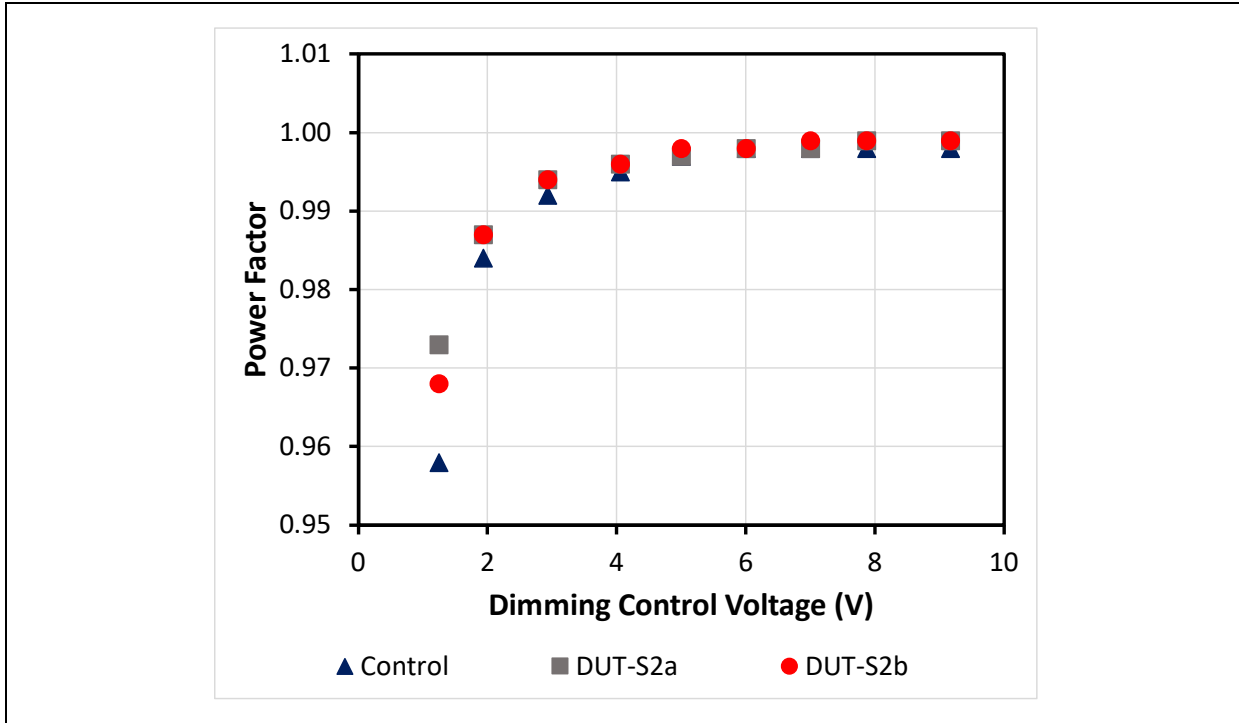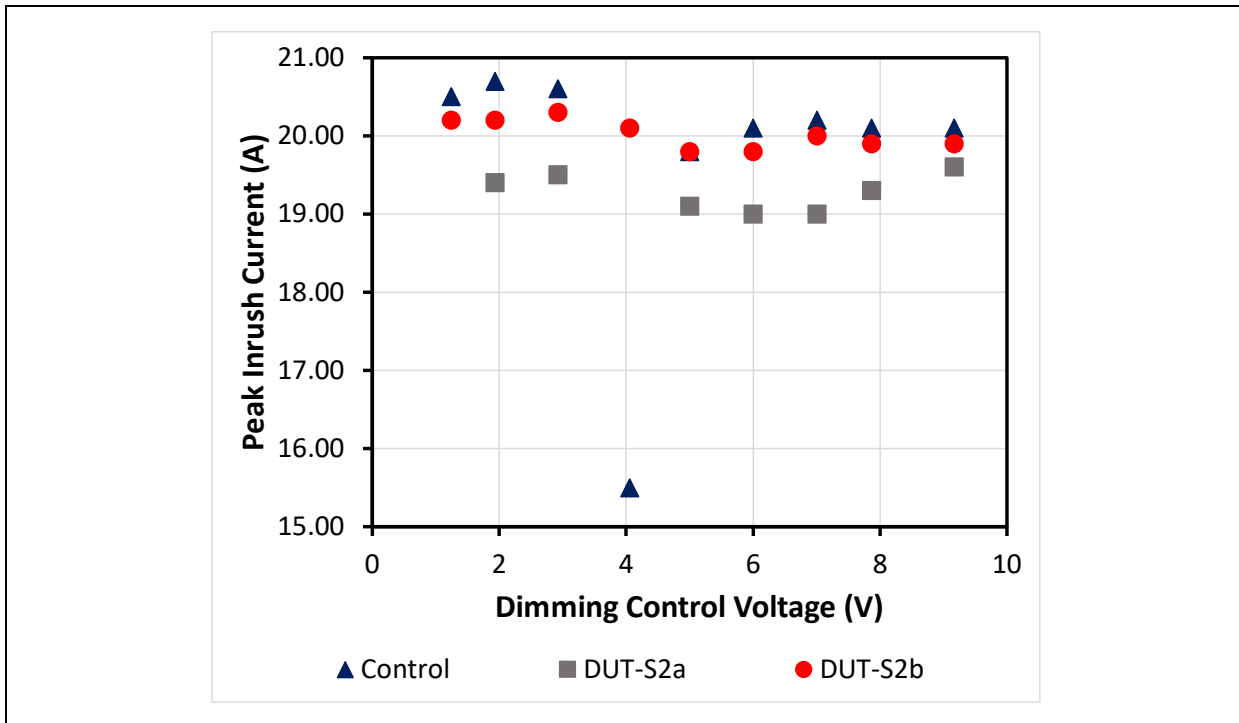

Figure 3-7. Peak inrush current, as a function of dimming control voltage, for the DUT-S2 control and samples DUT-S2a and DUT-S2b after exposure to 6,000 hours of testing in the 7575 environment.

Another method to measure the level of degradation in an SSL driver is to examine the change in photometric flicker as a function of exposure time in 7575 testing. Assuming there is no change in the LED load, which should be a reasonable assumption for the methods used in these tests, any changes in the photometric flicker response is caused by the driver. There are at least two scenarios where component degradation in the driver would cause flicker. The first scenario is degradation within the LED drive circuit itself. This circuit is typically a buck converter (see Figure 1-5), which means that degradation of the capacitor or the MOSFET could cause a change in flicker. The second scenario involves degradation in the Stage 1 circuits that provide power for the Stage 2 LED drive circuit. If these Stage 1 circuits are supplying incorrect or intermittent voltages, the LED drive circuit will not function properly, and photometric flicker could occur. For the DUT-S2 samples, there was no significant difference between the measured flicker response of either sample or the control as shown in **Table 3-4**. In general, the flicker response observed for both the 7575-exposed samples and the control was not periodic, so a flicker frequency could not be reliably calculated, and is not included in Table 3-4. However, both the % flicker and flicker index metrics provide evidence of minimal change in the waveforms supplied by the driver to the LED.

Table 3-4. Measured photometric flicker for the DUT-S2 samples.

	Dimming Control Voltage	% Flicker	Flicker Index
Control	1.25 V	0.6	0.0012
Control	10 V	0.2	0.0017
DUT-S2a	1.25 V	0.3	0.0007
DUT-S2a	10 V	0.2	0.0017
DUT-S2b	1.25 V	0.4	0.0009
DUT-S2b	10 V	0.3	

After 6,000 hours of exposure to the 7575 environment, both samples of DUT-S2 were still fully operational. Even though there were small changes in the PF and inrush current for these devices, the overall efficiency remained constant and the photometric flicker characteristics were largely unchanged. Together, these findings provide strong evidence that minimal degradation occurred in the LED drive circuit (i.e., Stage 2) and the Stage 1 circuits that feed the Stage 2 circuits in these samples even after 6,000 hours of exposure to 7575.

3.1.3   DUT-S3

The driver typology for DUT-S3 consists of flyback circuit in Stage 1 followed by a buck circuit in Stage 2. This device accomplishes light dimming using a CCR waveform with a small sinusoidal ripple. As a result, the % flicker of this device was slightly higher than DUT-S2 and varied between 3.6% at low dimming control voltage and < 1% at high dimming control voltages. The flicker frequency was nominally 120 Hz at all dimming levels, although higher harmonics appeared at the lower dimming levels.

Both of the DUT-S3 samples failed during testing in the 7575 environment (see Figure 3-1), and the electrical properties of the control and both 7575-exposed samples of DUT-S3 are given in **Table 3-5**. The failure of DUT-S3a involved the main fuse, so the device is completely non-operational. DUT-S3b exhibited intermittent operation after 3,658 hours of 7575 exposure, and this flickering behavior changed depending on the starting point for the dimming control voltage. Starting at the minimum dimming control voltage (1.35 V), DUT-S3b continuously operated when set to at low dimming levels (below 3.75 V); blinked at a low frequency (approximately 0.5 Hz) when set to medium (3.8 to 7.6 V) dimming levels; and flashed on, then off, and then remained on when set to at maximum output (i.e., 10 V dimming signal). If the dimming control voltage is set to 10 V when DUT-S3b is turned on, the device will start flickering when the dimming control voltage reaches 7.5 V and continues to flicker until the lowest dimming control voltage (1.34 V) setting is reached. The photometric flicker behavior at low dimming control setting (1.34 V) is shown in **Figure 3-8**. The photometric

flicker behavior at maximum output is shown for a long timescale in **Figure 3-9a** when the initial flash was observed and at a later time when the photometric flicker behavior has stabilized (**Figure 3-9b**). The temporal light artifacts associated with DUT-S3b were severe enough for it to be classified as a failure after 3,658 hours of 7575 exposure and it was removed from testing.

Table 3-5. Electrical properties of the failed DUT-S3 samples compared with the DUT-S3 control sample at maximum output

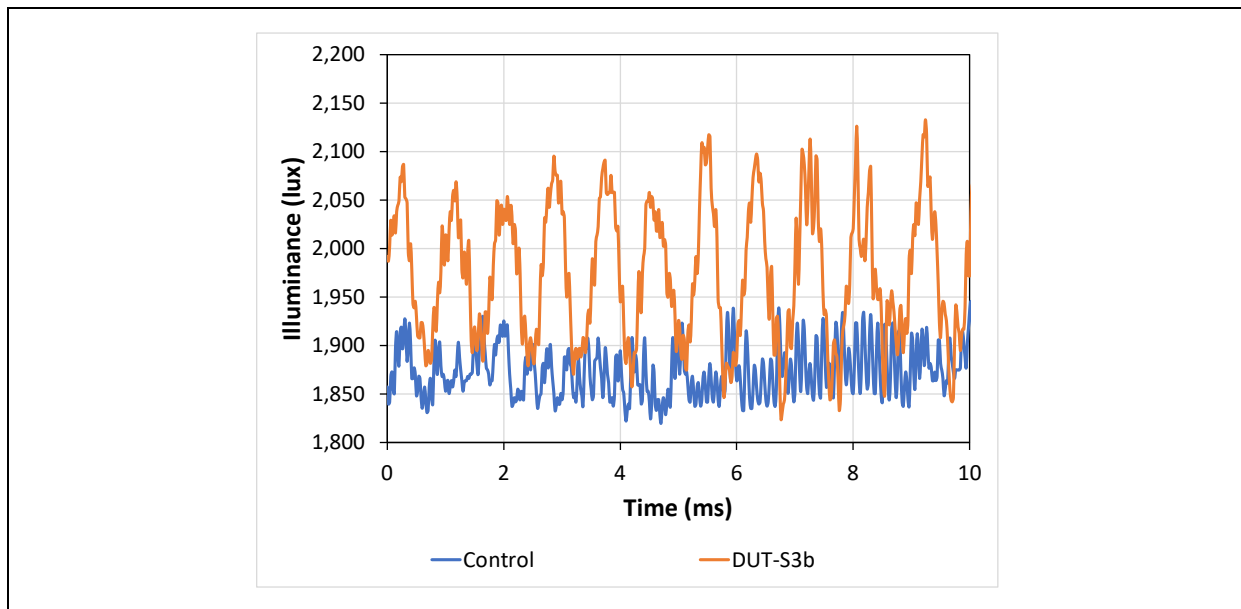| DUT-S3 Device	Input Current (mA)	Input Power (W)	PF
Control	490	59.01	1.00
DUT-S3a after 3,784 hours or 7575 exposure	0.00	0.00	0.01
DUT-S3b after 3,658 hours of 7575 exposure	580	68.61	0.98

Figure 3-8. Flicker measurements of the control and DUT-S3b at the low dimming setting.
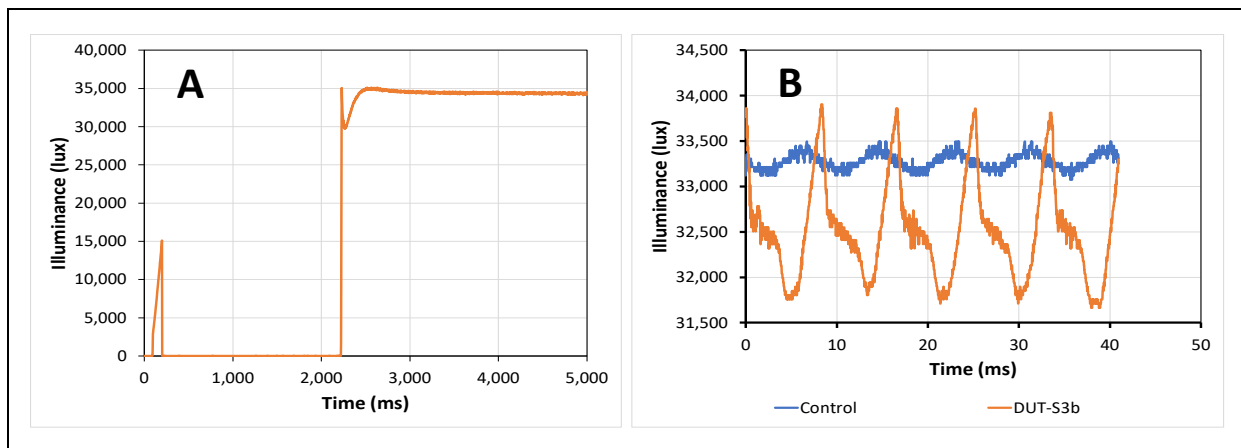
Figure 3-9. Flicker response of DUT-S3b at the maximum dimming level showing the device flickering on, then off, then back on (A) and the flicker characteristic after the device remains on (B).

The efficiency of DUT-S3b relative to the control varied greatly as a function of the dimming level, as summarized in **Table 3-6**. At the maximum light output setting, the efficiency of the control is significantly higher than that of DUT-S3b (post-7575 exposure), consistent with degradation of the device. However, the efficiency of DUT-S3b exceeds that of the control at the low dimming setting. Even though the efficiency of DUT-S3b increased at the low dimming control setting, the % flicker produced by the device also increased as shown in Figure 3-8. The electrical characteristics of the driver could not be accurately measured at intermediate dimming control voltages due to the flickering output of the driver. However, the photometric flicker response could be readily measured at medium dimming control settings and is shown in **Figure 3-10**.

Table 3-6. Electrical properties of the intermittently-failed DUT-S3b and the control sample at different dimming levels.

Dimming Signal	PF		Peak Inrush Current (mA)		Efficiency (%)	
	Control	DUT-S3b	Control	DUT-S3b	Control	DUT-S3b
10 V (max setting)	1.00	0.98	15,400	16,000	83.8	71.0
1.34 V (low setting)	0.95	0.99	15,400	930	45.6	49.9
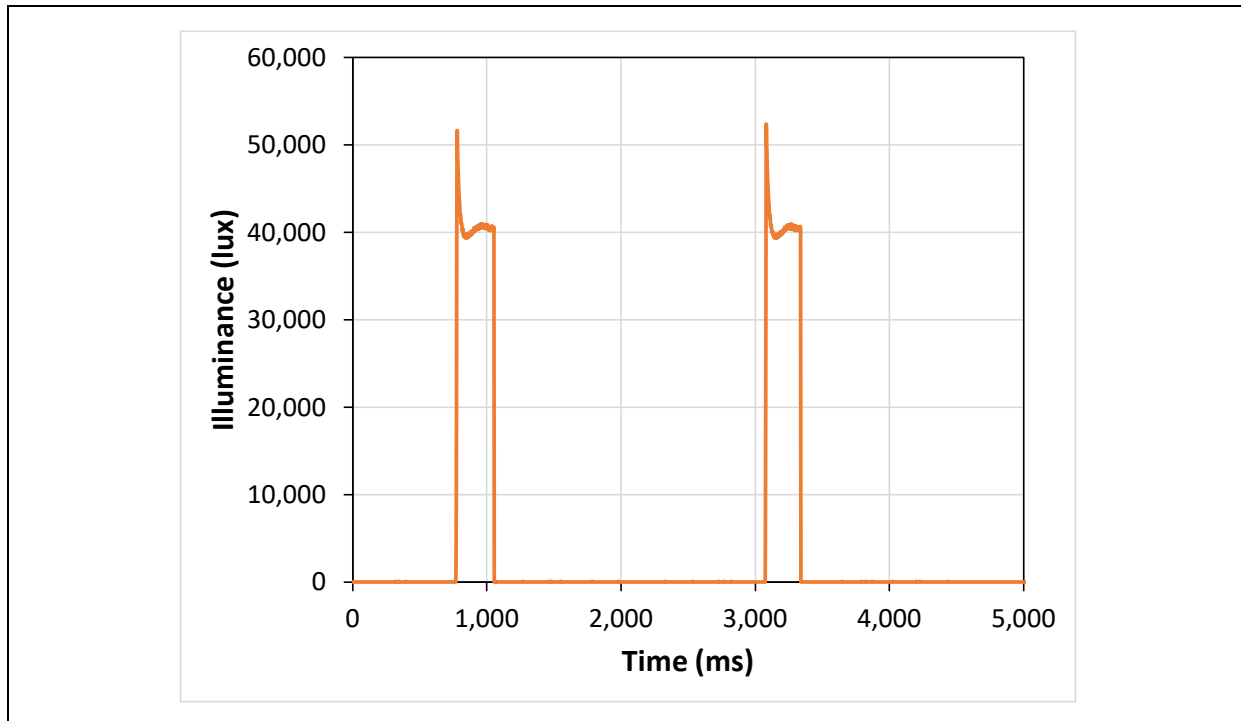
Figure 3-10. Response of the LED load connected to DUT-S3b at medium dimming level (5 V).

Given the nature of the intermittent failure observed for DUT-S3b, it can be concluded that the LED supply circuit (i.e., Stage 2) is functioning properly. This conclusion is supported by the fact that the device functions within specifications at low dimming control settings (see Figure 3-8) and at high dimming control settings after a short period (see Figure 3-9). Consequently, we assign the failure to Stage 1 of the device. Unfortunately, the potting on DUT-S3b made it difficult to locate the actual failure point.

3.2   Multichannel Drivers

Three different multichannel driver products, all capable of being used with TWL luminaires, were exposed to temperature and humidity environments for an extended time. The drivers were contained in an environmental chamber and attached to an external LED load that was placed outside the environmental chambers (see Section 2.1). The LED loads were chosen such that they required 95% of the maximum specified current for each driver. As there are a and b samples for each DUT, the individual samples are designated as DUT-M1a, DUT-M2a, DUT-M2b, and so forth. All three products were Class 2 devices that can operate at input ac voltages between 120 V and 277 V, although in this work, they were operated at 120 V. The three products were rated for surge protection of 2 kV. Specifications for these products are given in **Table 3-7** and additional information follows below.

Table 3-7. Manufacturer's specifications for the multichannel drivers examined in this study.

Driver No.	Output Voltage Range (V) Per Channel	Output Current Range (mA) Per Channel	Max Output Power (W)	Driver Efficiency	PF	THD @ Max Load	Max Case Temp °C
DUT-M1	30–54	700 typical	150	87%	>0.92	<20%	85
DUT-M2	2–55	200–1,050	50	89%	>0.9	<20%	85
DUT-M3	24	350–700	40		>0.9		90

[1] Values are given for 120 V operation only.

DUT-M1 was equipped with 0–10 V dimming and specified by the manufacturer to provide ingress protection (IP) equivalent to IP66. This driver has four channels and all four were operated during these tests. The driver utilized a CCR waveform with minimal flicker. The % flicker was 0.4% at high dimming control voltages and increased to 1.6% at the lowest (1.3 V) dimming control voltage. The interior of DUT-M1 was fully encapsulated with a hard, black plastic. The LED loads used on the two active channels of this driver were warm white and cool white LED modules, and the current required to operate these LEDs was approximately 95% of the specified load for each channel. The loads were mounted on aluminum heat sinks with separate dedicated warm white and cool white LED modules placed on separate heat sinks. The same loads were used during the 7575 testing and all post-testing electrical and photometric characterizations.

The DUT-M2 and DUT-M3 products were both dimmable using DMX controls, and both are rated for use in dry and damp locations. The flicker waveform for both devices transitions from a low % flicker, low frequency signal at high dimming settings (e.g., 100% setting on a DMX controller) to a high flicker % and high flicker frequency at lower dimming levels (e.g., less than 50% dimming setting on a DMX controller). The exact delineation between these regimes depends on both the dimming and CCT settings. Both products also had four output channels; however, only two channels were used for DUT-M2, whereas all four were used for DUT-M3. Equivalent loads were used for DUT-M2 and DUT-M3 although the load was distributed between two channels for DUT-M2 and four channels for DUT-M3. The warm white and cool white LED modules were housed on the same PCB but with separate connections to the driver. The interiors of both products were unencapsulated, allowing easy access for circuit analysis.

The operational lifetime of the different multichannel drivers is shown in **Figure 3-11.** Sample DUT-M1a failed early in the testing as reported previously [1]. Both samples of DUT-M3 failed in less than 4,000 hours of 7575 exposure [2], whereas both samples of DUT-M2 were still operational after 7,500 hours of exposure. Full details on the behavior of these devices are given in Section 3.2.1 for DUT-M1, Section 3.2.2 for DUT-M2, and Section 3.2.3 for DUT-M3.
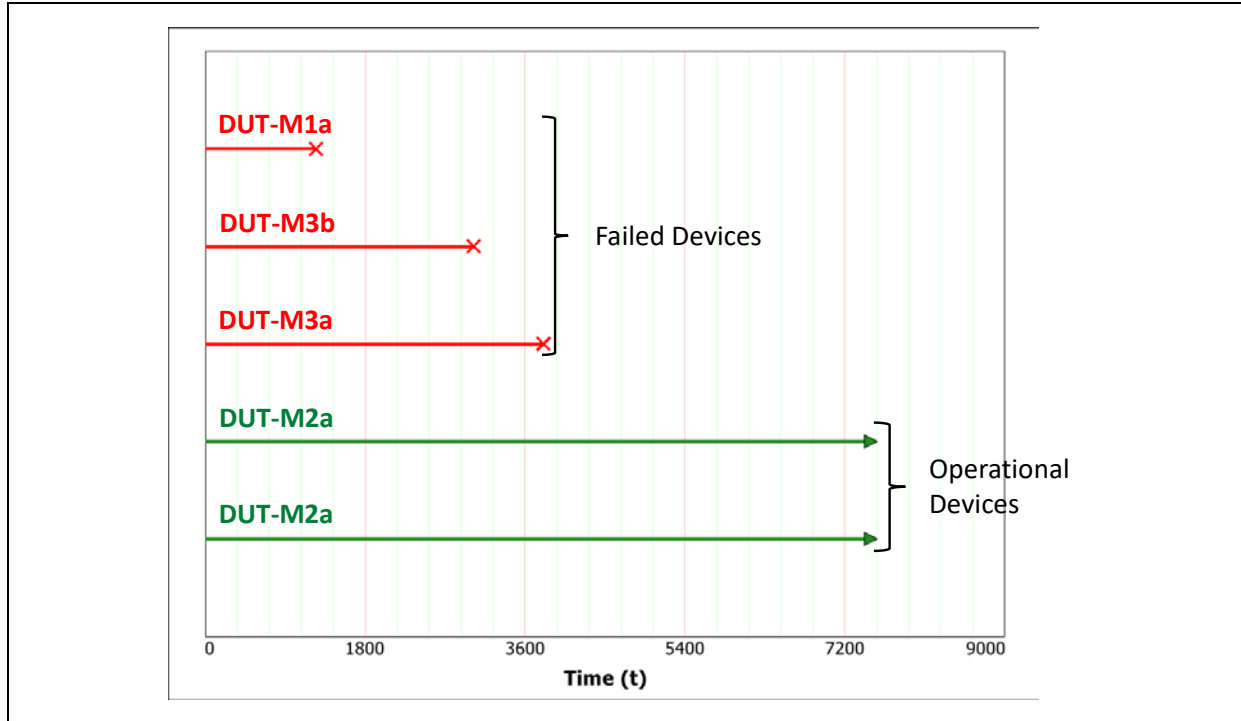
Figure 3-11. Functional status (red = failure, green = operational) and operational time for the multichannel drivers subjected to 7575 testing.

A Weibull analysis was also performed on the 7575 data for the multichannel drivers, and the Weibull plot is shown in **Figure 3-12**. The 90% confidence interval for this plot is larger than that observed for the single-channel drivers (see Figure 3-3) likely reflecting the smaller sample size and the larger range of operational times.

Figure 3-12. Two-parameter Weibull plot for the multichannel drivers subjected to 7575 exposure.

3.2.1 DUT-M1

DUT-M1 is a four-channel driver intended for use in outdoor luminaires. The basic structure of the driver is a combination of PFC and inductor-inductor capacitor (LLC) converter circuits in Stage 1 to produce the intermediate dc power, which is then fed to Stage 2 and its control IC and on to separate buck inductors for each LED primary. Interactions between the control ICs and the different power conversion circuits help to control the overall output waveform provided to the LED load. Only one sample of DUT-M1 was tested in 7575 because of its high power output. As previously reported, testing of this device (DUT-M1a) was terminated after 1,250 hours when the power consumption and light output dropped precipitously, and the device was classified as a failure [1, 2]. However, the device was still consuming power when removed from testing, albeit at a significantly lower rate than when fully operational. Failure of DUT-M1a was attributed to failure of the film capacitors in the resonant circuit of the LLC converter that also caused the MOSFET in this circuit to fail [1]. No further analysis was performed on this sample.

3.2.2 DUT-M2

DUT-M2 is a four-channel driver intended for use in indoor or outdoor luminaires. For the 7575 exposure tests, only two channels were used. The basic structure of the driver comprises a combination of PFC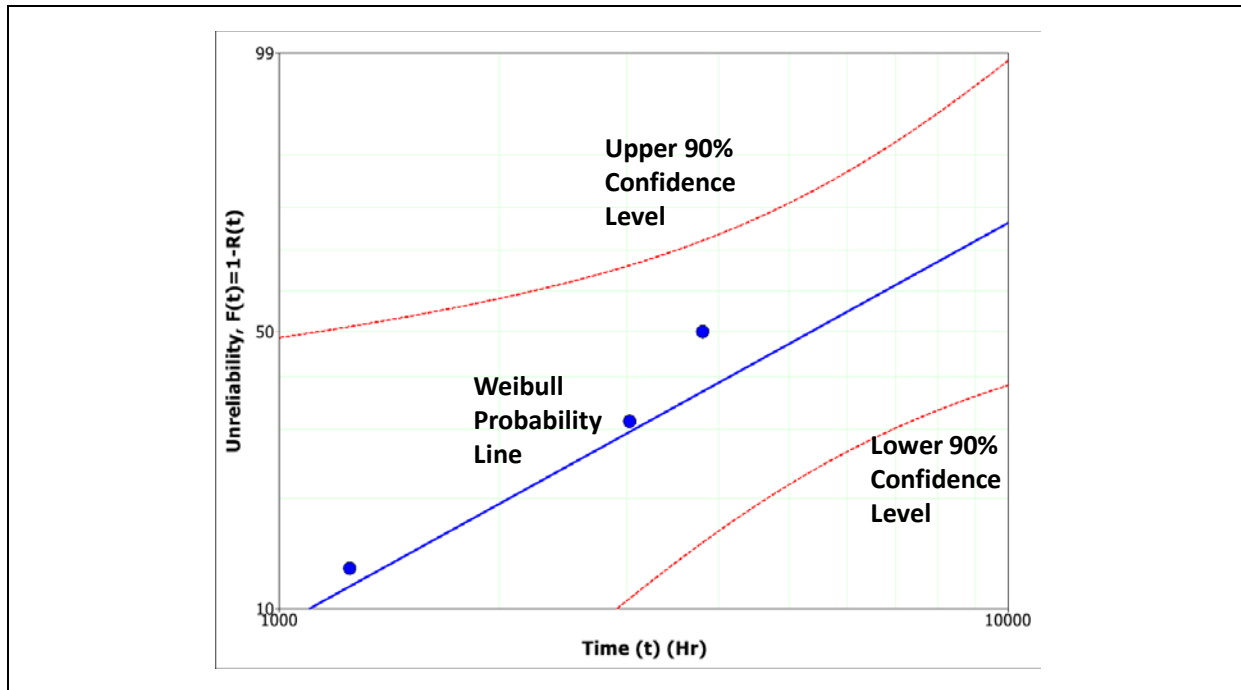 and LLC converter circuits in Stage 1 to produce intermediate dc power, which is then downconverted and distributed through a control IC to separate buck inductors for each channel.

Both DUT-M2 samples were still operational after 7,500 hours of exposure to the 7575 environment, so a suite of electrical and photometric characterizations were performed to gauge the extent of any degradation that occurred during exposure. This analysis consisted of several steps. First, the average input and output power of the two samples were compared to the values for a control sample that was not subjected to 7575 exposure. As shown in **Table 3-8**, both the input power consumption and delivered output power were generally higher in the samples exposed to the 7575 environment, compared to the control.[2] On the input side, the power consumption increased by 3-7% depending on the dimming level, whereas on the output power side, the power delivered to the LED load increased by less than 2% to the 50% dimming setting. A slight decrease in the output power delivered to the LED load was found when the dimming level was set to 25% or 1%.

Table 3-8. Average input and output power of the test 7575 DUT-M2 devices after 7,500 hours exposure compared with the input and output power of the control DUT-M2 device.

Dimming Level (%)	Input Power		Output Power	
	Control (W_{ac})	7575 Samples Average[a] (W_{ac})	Control (W_{dc})	7575 Samples Average [a] (W_{dc})
100[b]	49.16	50.45	41.89	42.58
75	26.65	27.85	21.48	21.86
50	14.35	15.34	10.11	10.24
25	6.47	6.77	2.77	2.67
1	2.78	2.91	0.30	0.27

[a] These values are the average input and average output power of DUT-M2a and DUT-M2b after 7,500 hours of operation in the 7575 environment.

[b] A dimming level of 100% indicates that no dimming was applied.

The efficiencies of the control driver and both samples subjected to 7575 exposure are shown in **Table 3-9** at different DMX dimming levels. The slight variations in output current and voltage led to marginally lower driver efficiencies for the samples exposed to 7575 compared to the control device at all dimming levels except

---

[2] NOTE: Equivalent LED loads were used in the testing.

25% and 1%. These changes in the electrical performance of the DUT-M2 samples suggest some degradation following 7575 exposure. However, the changes were relatively small given the overall performance of the exposed samples.

Table 3-9. Efficiencies, at various dimming levels, of the DUT-M2 control and both DUT-M2 samples after exposure to 7,500 hours of 7575[a]

Dimming Level (%)	Control	DUT-M2a	DUT-M2b
100[b]	84.6%	83.9%	84.1%
75	79.4%	78.1%	77.9%
50	67.6%	66.8%	65.3%
25	36.0%	39.3%	36.6%
1	5.1%	7.1%	5.6%

[a] The power required to operate the DMX controller is not included in the efficiency calculation.

[b] A dimming level of 100% indicates that no dimming was applied.

The change in PF value, as a function of exposure time to the 7575 environment and dimming levels, was also studied and the results are presented in **Figure 3-13** for DUT-M2a. Clearly the device PF decreases as a function of dimming level even in the control. However, the PF value increased as a function of time in the 7575 environment, and this effect is especially pronounced at dimming levels below 50%. The capacitance of the film capacitors used in the EMI filter were examined to help explain the rise in the PF value. As shown in **Table 3-10**, the EMI filter capacitors tended to drop in capacitance as cumulative exposure to the 7575 environment increased. In addition, it is also highly likely, although not measured, that the ESR of these capacitors also increased, changing the load into one with the characteristics of greater resistance [17]. These findings are consistent with an increase in power consumption and higher PF values, as observed here, as the components age.
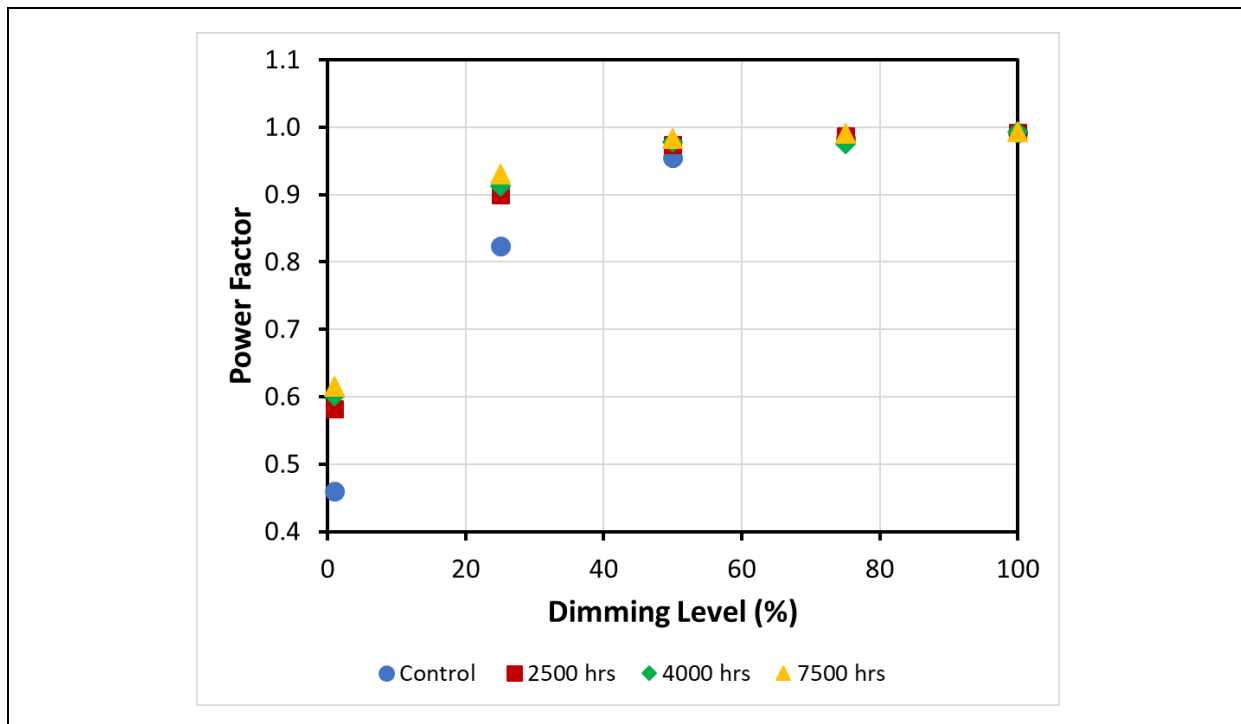

Figure 3-13. The PF of DUT-M2a continued to increase at low dimming levels as cumulative exposure to the 7575 environment increased.

Table 3-10. Change in capacitance of EMI filter components in the DUT-S2 control and samples.

Device	After 2,500 Hours of 7575 Exposure		After 4,000 Hours of 7575 Exposure		After 7,500 Hours of 7575 Exposure	
	Capacitor C_5 (nF)	Capacitor C_6 (nF)	Capacitor C_5 (nF)	Capacitor C_6 (nF)	Capacitor C_5 (nF)	Capacitor C_6 (nF)
Control	429.0	429.0	413.5	413.5	363.9	363.9
DUT-M2a	258.6	258.6	235.9	235.9	2.9	2.9
DUT-M2b	314.6	314.6	258.4	258.4	192.8	192.8

A comparison of the electrical characteristics (input volts, input current, input power, and inrush peak current; output volts, output current, and output power; and PF) of the control and sample devices is consistent with the finding of minimal degradation of DUT-M2a and DUT-M2b during operation in the 7575 test conditions. There was, however, a difference in the inrush peak current for the samples exposed to 7575 test conditions compared to the control device. As shown in **Figure 3-14**, the inrush peak current of the 7575-exposed DUTs was consistently lower than that of the control device across the dimming range. The lower inrush peak current likely stemmed from higher impedance within the device, possibly because of higher ESR in the EMI filter capacitors, and suggests that some degradation occurred within the samples exposed to 7575. Electrical measurements also revealed slight differences in the input power and output power for each channel between the control and sample devices; these differences represented a combination of slight variations in voltage and current, but are not generally large.
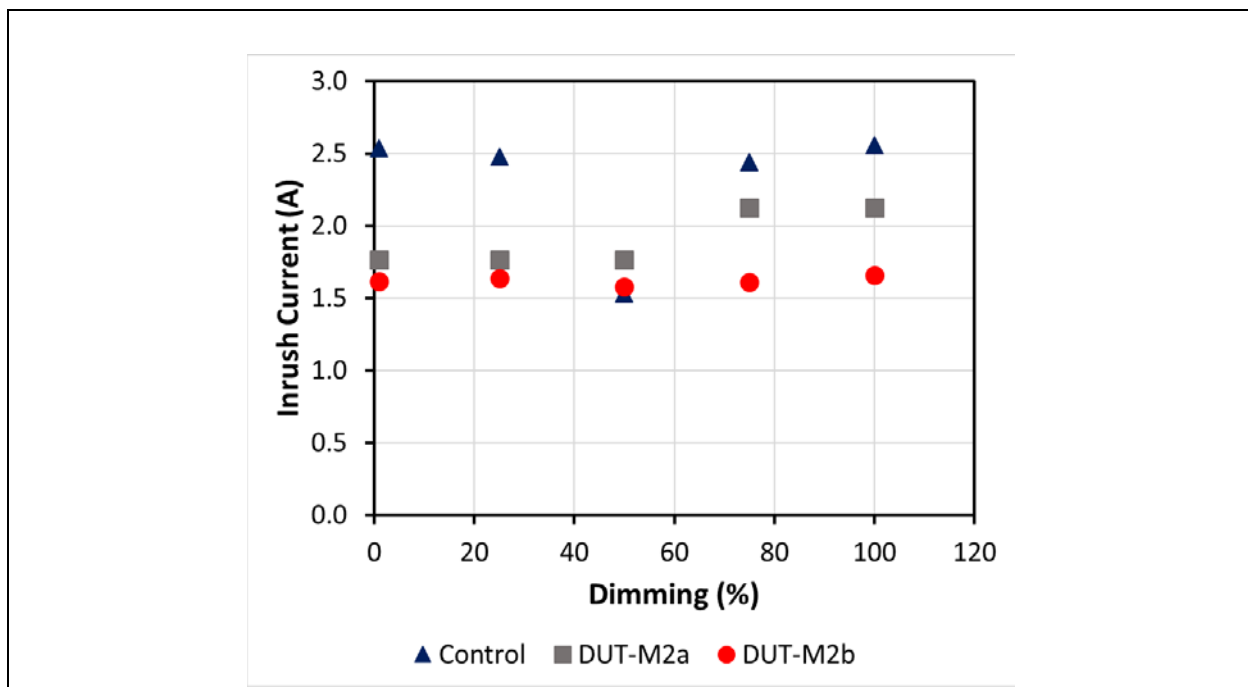
Figure 3-14. Comparison of the inrush current of the 7575-exposed samples and the control.

Additional insights into the degradation of the two samples of DUT-M2 exposed to the 7575 environment can be gained by comparing the photometric flicker of LED loads attached to these samples to that of the control device. Because the flicker of the LEDs could be influenced by any changes in the circuit that delivers current to the LEDs, this measurement provides a direct status monitor of the LED drive circuit. As shown in **Figure 3-15**, the waveforms of the 7575-exposed samples and the control are very similar; however, the data suggest that the resistor-capacitor (RC) time constant of the control is slightly larger than that of either sample, which

could indicate a slight change in the LED drive circuit as a result of exposure. The data are shown for a CCT value of 6,500 K and a dimming level of 1% due to the simplicity of the waveform at this setting as only one LED primary is active. Similar results were also found at 2,700 K (when only the warm white primary is active) and at 3,500 K when both sets of LED primaries are active. Overall, the change suggested by the photometric flicker measurements is small, in agreement with findings from the electrical tests.

Figure 3-15. Photometric flicker waveforms for DUT-M2a, DUT-M2b, and the DUT-M2 control set to 1% dimming and a CCT of 6,500 K. The measurements were taken after 7,500 hours of 7575 exposure for DUT-M2a and DUT-M2b.

3.2.3   DUT-M3

DUT-M3 is a two-stage four-channel driver with a flyback PFC converter for Stage 1 and separate buck circuits for each channel in Stage 2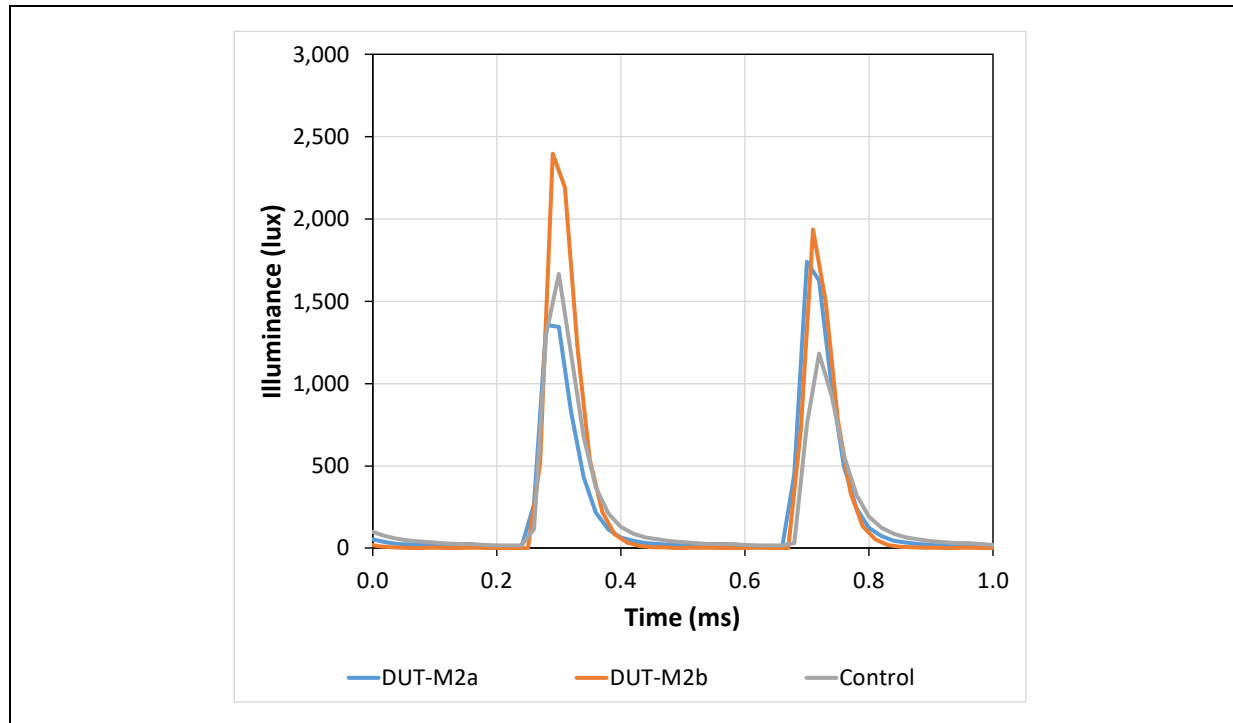. In this device, the Stage 2 MOSFETs are integrated into the Stage 2 control IC, whereas in the other drivers, the Stage 2 MOSFETs and control IC are separate components. Both samples failed during 7575 testing, with DUT-M3a failing at 3,812 hours and DUT-3b failing at 3,027 hours. In our previous reports, the reliability of DUT-M3 was extensively presented including a detailed failure analysis [2]. In summary, device failure was traced back to multiple components in the PFC circuit in Stage 1, including the Stage 1 MOSFET (in one instance) and open capacitors and a blown fuse in the other [2]. Prior to failure, minimal changes were observed in the electrical characteristics—although there was an increase in PF at low dimming levels due to aging of film capacitors in the filter and conditioning circuit [2]. This increase in PF is the same as that observed for DUT-S2 and DUT-M2.

Photometric flicker studies were performed on both DUT-M3a and DUT-M3b throughout 7575 exposure, and a comparison of the flicker waveform at 50% dimming and a CCT setting of 3,500 K is given in **Figure 3-16**. Because there are two LED primaries, the CCT level is determined by the relative pulse-width and peak intensity of each. As shown in Figure 3-16, the total illuminance in one cycle (flicker % is 99% and flicker frequency is 1,446 Hz) consists of two light pulses, one on top of the other. Using the Fluke ScopeMeter, we traced these two light pulses in each cycle to the LED primaries. At a CCT value of 3,500 K, the pulse-width of the warm white primary is longer (duty cycle is approximately 70%), while the shorter pulse-width of the cool white primary can be seen as the smaller, separate peak on top of the warm white peak (duty cycle is

approximately 25%). The overall peak height of light emissions from the warm white and cool primaries is similar, but the peak width of light emissions from the warm white primary is wider indicating that more optical power is delivered by this channel. At higher CCT values, these ratios change with the peak-width of the cool white channel becoming relatively longer as CCT increases.
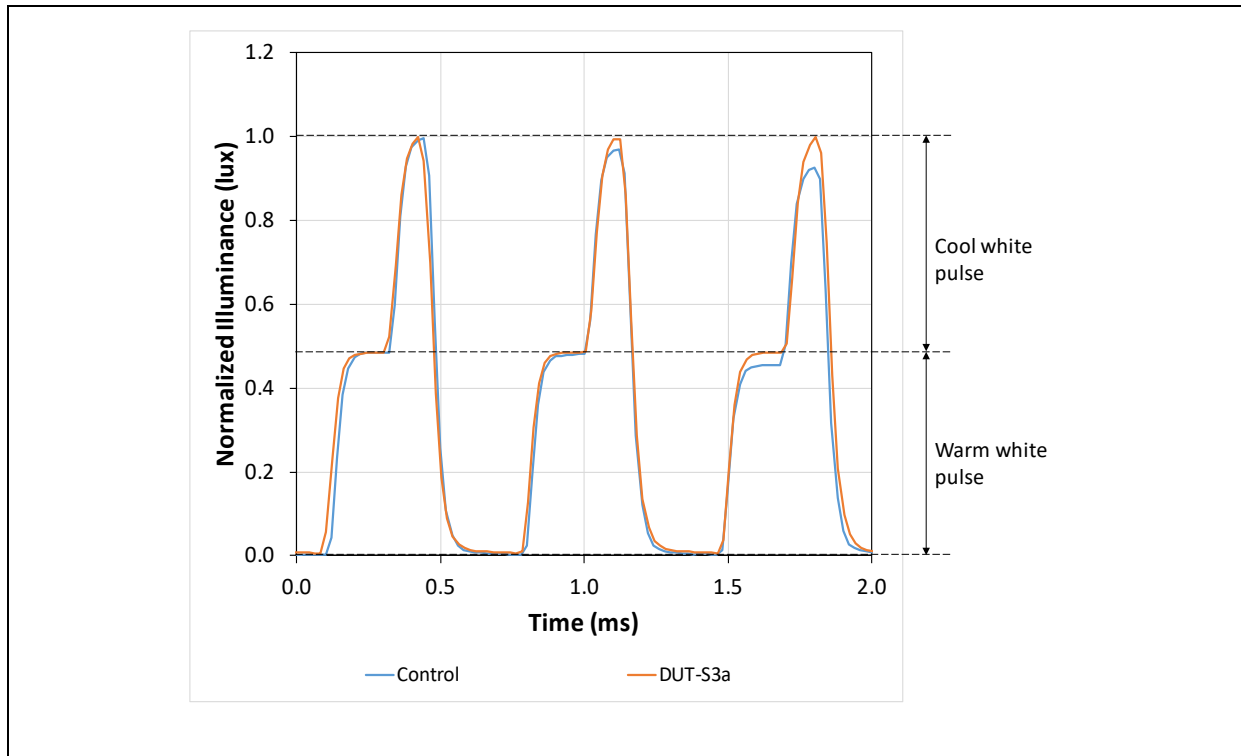
Figure 3-16. Comparison of the photometric flicker waveform for DUT-M3a (after 3,750 hours of 7575 exposure) and the DUT-M3 control. Measurements were taken at 50% dimming and CCT = 3,500 K.

To provide a TWL spectrum, the buck circuit in the DUT-M3 samples must be able to accurately control peak width, peak height, and pulse timing regardless of the level of degradation in the buck circuit driving the LEDs. The data shown in Figure 3-16 for DUT-M3a was taken after 3,750 hours of exposure to the 7575 environment and roughly 62 hours before device failure. The difference in peak shape between DUT-M3a and the control is minimal, indicating no significant change in the electrical components comprising the buck circuit, even at this later stage of useful life.

4 Conclusions

Eleven different two-stage drivers were subjected to a 50% power cycle test while operating in a 7575 temperature and humidity environment. During these tests, only the drivers were contained in the temperature–humidity chamber (where they were exposed to 7575) while external LED loads were placed outside the chamber. Consequently, failure of these devices can be attributed to changes in the driver, not the LED loads. This testing environment was chosen in order to stay within maximum case temperature requirements from the manufacturers (see Table 3-1 and Table 3-7) and because these conditions have been shown useful for accelerating the failure of SSL downlights [20].

Of the 11 driver samples, 7 failed (64% failure rate) in less than 4,800 hours of testing, with failure times ranging from 1,250 hours to 4,554 hours (see Figure 3-1 and Figure 3-11). All of the failures can be traced to circuits involved in providing PFC, EMI suppression, and intermediate dc voltages within the samples. None of the failures were traced back to the circuits directly driving the LEDs. The capacitors in the EMI filter in Stage 1 seemed to be the most susceptible to failure in the 7575 environment, although other components such as fuses, switching MOSFET transistors, and feed resistors were also found to fail. Complete details of the failure analysis can be found in Sections 3.1 and 3.2 of this report, and in our earlier reports [1, 2]. In a few cases, the level of photometric flicker became so severe that the device was not functioning properly and we classified it as a failure, although it was still producing light. Based on this analysis, it appears that the outcome of 7575 testing is to degrade the Stage 1 circuits (e.g., PFC, EMI suppression) supplying the LED drive circuit in Stage 2, producing a malfunction that affected the electrical waveforms fed to the LEDs. This malfunction may have produced an undervoltage situation where there was insufficient electrical voltage to turn on the LEDs, but power was still being consumed in the circuit (even after failure), affecting the lifetime energy efficiency of the device. In some instances, the LED drive circuit can function for an intermittent period but becomes unstable and produces photometric flicker.

MOSFETs have also been found to cause "lights-out" failure in SSL devices, and MOSFET failure has been observed to produce cascade failures in capacitors and other components in SSL devices presumable due to large current surges [18, 20]. In general, two-stage drivers will have multiple MOSFETs. There is usually one MOSFET associated with the Stage 1 circuit (e.g., flyback or boost) and one MOSFET for each buck circuit in Stage 2. In these tests, there were three confirmed MOSFET failures (DUT-S1a, DUT-M1a, DUT-M3b), and all of these failures are associated with Stage 1 circuits. The products we examined in this study used different methods to manage the heat generated by a MOSFET and other circuit components. DUT-S1, DUT-S3, and DUT-M1 used a thermal potting compound to spread excess heat among all components. This thermal compound was not able to prevent early failure in these devices, as each failed in less than 4,800 hours of 7575 exposure. In contrast, both samples of DUT-S2 and DUT-M2 survived 6,000 hours and 7,500 hours, respectively, in 7575 before their testing was terminated. Both of these products took steps to transfer heat generated by the MOSFETs to the driver case for dissipation. DUT-S2 uses thermal pads to establish a direct thermal link between the MOSFETs and the case, while DUT-M2 uses heat sinks and thermal pads attached to the main MOSFETs to transfer heat to the case. None of the failed devices had this level of heat management. This finding suggests that proper heat management in MOSFETs and other components (e.g., inductors and transformers, capacitors) is important to achieving higher reliability in SSL devices.

Based on these testing data, a combined Weibull analysis was performed on all the LED drivers (i.e., both single-channel and multichannel drivers) and the outcome is shown in **Figure 4-1**. The basic trends are similar to those shown in Figure 3-3 for the single-channel drivers, although the β and η values are slightly lower. To some extent, the lower values in this analysis are driven by the early failure of DUT-M1a, although there is some uncertainty in the exact β and η values, as shown by the confidence interval, so the differences in the values may be negligible. In the combined single-channel and multichannel driver analysis, the characteristic life (i.e., Weibull η value) in 7575 was 5,056 hours and the Weibull β value was 2.30, indicating an accelerating failure rate. The drivers used in this analysis represented six different manufacturers; therefore, the findings can be taken as an industry benchmark.
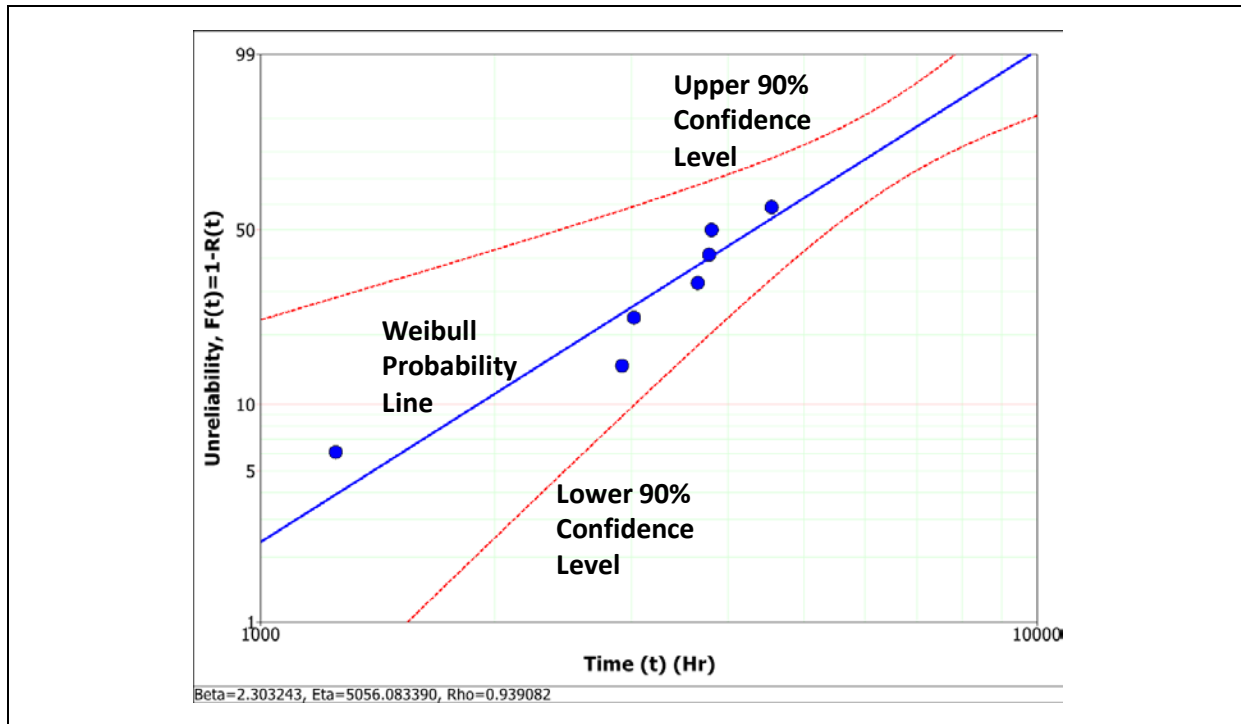
Figure 4-1. Complete Weibull analysis for all the drivers subjected to the 7575 environment during extended power cycling.

Previously, the robustness of 6" downlights was tested in several different temperature–humidity environments including 7575 [20]. As with the drivers examined in this report, the 6" downlight samples were chosen from an assortment of manufacturers (8 in all) and the findings are assumed to be representative of the available products. The Weibull plot of the 6" downlight findings from this earlier study in 7575 is given in **Figure 4-2** [20]. The characteristic life (i.e., Weibull η value) was calculated as 5,421 hours, while the β value was calculated to be 1.30. In comparison with the driver samples, the η values differ by less than 7% suggesting good correlation, while the β values differ by more than 40%. The reason for this difference in β values is currently not known and deserves additional investigation.

The Weibull plot for the drivers examined in this study can also be compared with that of the Hammer Test. Recently, the original Hammer Test data of the 6" downlights with two-stage driver configurations were reviewed and classified by driver type (i.e., single-stage and two-stage drivers), and the Hammer Test Weibull plot updated [2]. This updated plot is provided in **Figure 4-3** for convenience. The Weibull slope (i.e., β value) of the updated analysis for the Hammer Test is much steeper than that of driver testing (4.66 vs. 2.30), indicating that the Hammer Test is more accelerating than 7575 alone. In conjunction with the large β value, the characteristic life (η value) dropped to 1,040 hours in the Hammer Test, much lower than that found in temperature and humidity testing alone. We attribute both of these findings to the extreme conditions of the Hammer Test, especially the temperature shock cycling and the use of a more severe temperature–humidity environment of 85°C and 85% relative humidity [26]. This finding is also reflected in the different failure modes observed in the two tests. The Hammer Test produced a greater incidence of solder joint failures, likely due to the temperature shock cycle, whereas this failure mode was not observed in this test.
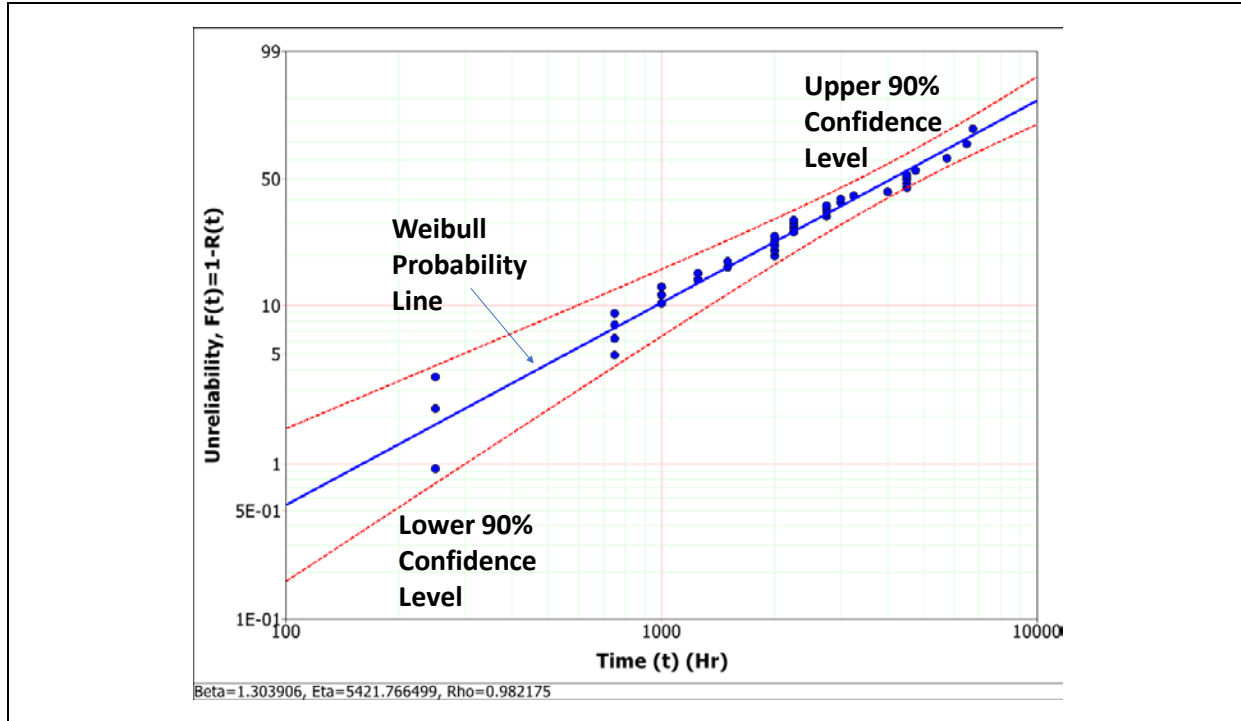
Figure 4-2. Weibull analysis of 6" downlights exposed to 50% power cycling in a 7575 environment (from [19]).
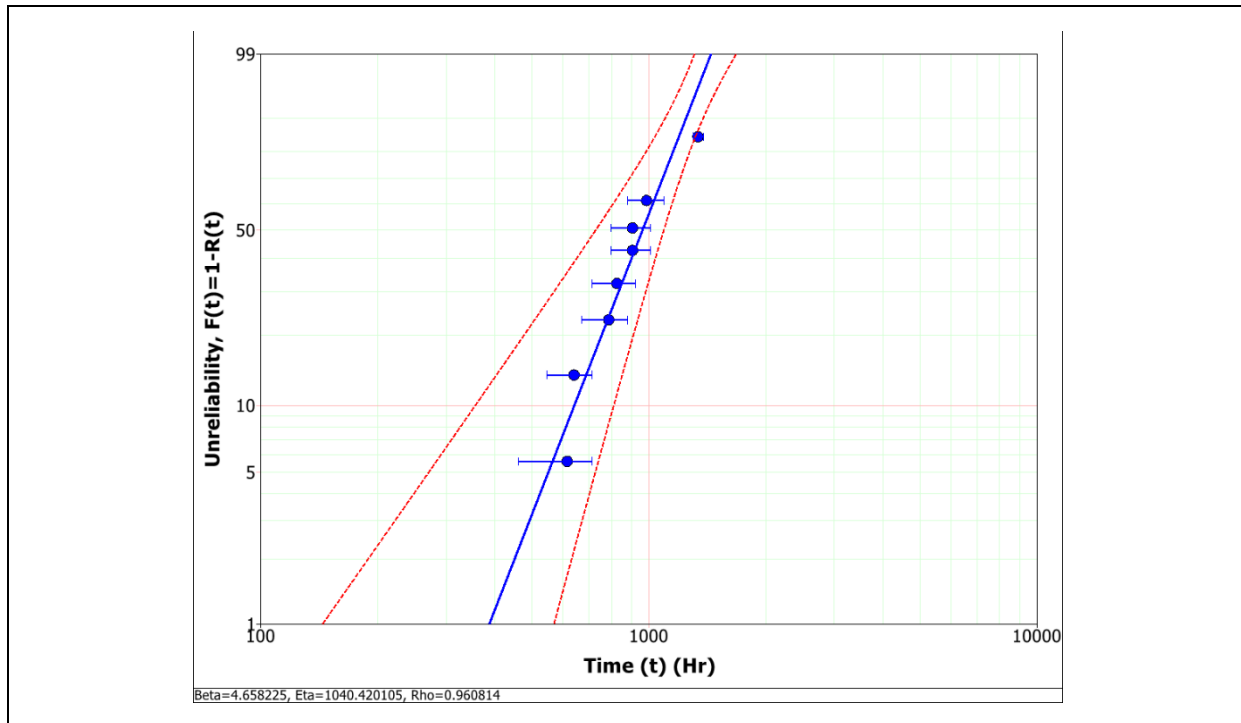
Figure 4-3. Updated analysis for the Hammer Test to include only devices with two-stage drivers [2].

While the majority of the drivers examined in this study failed during 7575 testing, there were early indications in all drivers of device degradation in the EMI and PFC circuits. Most notably, the film capacitors used in the EMI filter changed quickly, resulting in a noticeable shift in PF (especially at low dimming levels). In addition, inrush currents and device efficiency also changed during 7575 exposure. These changes are likely driven in

part by the higher voltages that film capacitors experience in these electrical circuits because voltage, temperature, and humidity are accelerating factors for capacitor degradation [17]. In addition, the application of an ac voltage has been found to increase the degradation of film capacitors [14]. Upon rectification, the peak voltage in the EMI and PFC circuits can be as high as 170 V (assuming a 120 V_{ac} root mean square on the electrical mains). As the circuit elements in this part of the device must withstand this voltage for the device to operate properly, film capacitors with higher voltage ratings are typically used. Power quality, especially transients and voltage surges, is a major concern and will degrade in the Stage 1 circuits over time as the EMI suppression filter degrades. As a result, the adverse impact of electrical transients will increase and affect overall circuit performance.

In contrast, the film capacitors on the LED drive circuits did not experience the same level of degradation, as evidenced by analysis of the flicker waveforms, even though they were operating in the same 7575 environment. We attribute this finding to the fact that the LED drive circuit, which is typically a buck converter, generally has a cleaner power supply with fewer electrical transients than the other parts of the circuit. In addition, the operational voltage of the buck circuit is lower than in the Stage 1 circuitry, which generally increases the lifetime of capacitors [17, 20].

Combined, these findings lend support to the use of 7575 as a means to assess the robustness of SSL drivers and fixtures. There were some similarities in behavior of drivers and 6" downlights subjected to 7575 exposure. In particular, both SSL devices exhibited similar characteristic lifetimes in this test, although the Weibull slopes were different. While performing 7575 tests to failure is beneficial to understanding the full robustness of the DUTs, early indications of their long-term performance can be gathered from the temporal changes in electrical parameters such as PF, inrush current, and efficiency. Monitoring of these changes can be used as a measure of residual life in real-time monitoring of SSL devices. Alternatively, this same characteristic can be used in AST of SSL devices to provide an early indication of robustness, without the necessity of operating the DUTs to complete lights-out failure.

These tests also provide an indication of methods that can be used to improve the reliability of SSL drivers. Specifically, more attention should be paid to the circuits involved in filtering the incoming power and controlling emissions from SMPSs including the EMI suppression filters and the methods used to provide PFC. Both of these functions often occur after the diode bridge in the ac rectification circuit, although sometimes the EMI suppression circuit is split on either side of the diode bridge. Improving the performance of these devices, through new designs or improved part selection, should provide additional gains in the robustness of SSL drivers.

References

1. Davis, L., Rountree, K., Mills, K., & Athalye, P. (2018). *Accelerated stress testing on single-channel and multichannel drivers.* Washington, DC: U.S. Department of Energy. Available from https://www.energy.gov/sites/prod/files/2018/06/f53/rti-ssl_multichanneldriver_initial-results.pdf.

2. Rountree, K., Davis, L., & Mills, K. (2018). *Accelerated stress testing on multichannel drivers – updated test results*. Washington, DC: U.S. Department of Energy. Available from https://www.energy.gov/sites/prod/files/2018/07/f53/ssl_ast-multichannel-updated-results_may18.pdf.

3. Zhao, M., Zhang, D., Zhou, Z. Li, T., & Wang, Z. (2015). Novel method for failure prognostics of power MOSFETs. 2015 IEEE International Conference on Computational Intelligence and Virtual Environments for Measurement Systems and Applications (CIVEMSA). Shenzhen, China. doi: 10.1109/CIVEMSA.2015.7158628.

4. Miller, N.J. (2018). "Flicker: How to avoid it, test for it, and fix it." Presentation at LightFair International 2018. Chicago, IL. May 9, 2018. Available from https://www.energy.gov/sites/prod/files/2018/05/f51/lfi2018_miller_0.pdf.

5. Pacific Northwest National Laboratory. (2016). *CALiPER Report 23: Photometric testing of white-tunable LED luminaires.* Report Number PNNL- 24595. Washington, DC: U.S. Department of Energy. Available from https://energy.gov/sites/prod/files/2016/01/f28/caliper_23_white-tunable-led-luminaires.pdf.

6. Clark, T. (2016, November 21). Future-proof tunable white lighting is a smart choice for classrooms. *LEDs Magazine*, *13*. http://www.ledsmagazine.com/articles/print/volume-13/issue-9/features/tunable-lighting/future-proof-tunable-white-lighting-is-a-smart-choice-for-classrooms

7. Davis, J. L., Mills, K., Hensley, E., Clark, T., & Smith, A. (2017). *Luminaires for advanced lighting in education. Final report of DOE project DE-EE0007081*. Washington, DC: U.S. Department of Energy. DOI: 10.2172/1367149. Available from https://www.osti.gov/scitech/servlets/purl/1367149.

8. Davis, R. G., & Wilkerson, A. (2017). *Tuning the light in classrooms: Evaluating trial LED lighting systems in three classrooms at the Carrollton-Farmers Branch Independent School District in Carrollton, TX. Report Number PNNL-26812.* Washington, DC: U.S. Department of Energy, 2017. Available from https://energy.gov/sites/prod/files/2017/10/f37/2017_gateway_tuning-classroom_0.pdf.

9. Safranek, S.F., & Davis, R.G. (2018). *Evaluating tunable lighting in classrooms: Trial LED lighting systems in three classrooms in the Folsom Cordova Unified School District. Report Number PNNL-27806.* Washington, DC: U.S. Department of Energy. Available from https://www.energy.gov/sites/prod/files/2018/09/f56/2018_folsom_classroom-tunable%20lighting.pdf.

10. Davis, R. G., Wilkerson, A. M., Samla, C., & Bisbee, D. (2016). *Tuning the light in senior care: Evaluating a trial LED lighting system at the ACC Care Center in Sacramento, CA. Report Number PNNL-25680.* Washington, DC: U.S. Department of Energy. Available from https://www.energy.gov/sites/prod/files/2016/09/f33/2016_gateway-acc.pdf.

11. Wilkerson, A., Davis, R. G., & Clark, E. (2017). *Tuning hospital lighting: Evaluating tunable LED lighting at the Swedish Hospital Behavioral Health Unit in Seattle. Report Number 26606.*

Washington, DC: U.S. Department of Energy. Available from https://www.energy.gov/sites/prod/files/2017/08/f36/2017_gateway_swedish-tuning-led_0.pdf.

12. Winder, S. (2017). *Power supplies for LED driving, Second Edition*. Oxford, England: Newnes. ISBN: 9780081009253.

13. Wang, Y., Alonso, J.M., Ruan, X. 2017. A review of LED drivers and related technologies. *IEEE Transactions of Industrial Electronics* vol. 64, no. 7, pp. 5754 – 5765. Doi: 10.1109/TIE.2017.2677335.

14. Shaw, D.G., Cichanowski, S.,W. Yializis, A. (1981). A changing capacitor technology – failure mechanisms and design innovations. *IEEE Transactions on Electrical Insulation* vol. EI-16, no. 5, pp. 399-413. doi: 10.1109/TEI.1981.298435.

15. Keebler, P.F. and Phipps, K.O. 2007. Power quality effects on the reliability and susceptibility of EMI filters. *Interference Technology.* Available at: https://interferencetechnology.com/power-quality-effects-reliability-susceptibility-emi-filters/.

16. Keagy, M. 2002. Calculate dissipation for MOSFETs and high-power supplies. *Electronics Design.* Available at: https://www.electronicdesign.com/boards/calculate-dissipation-mosfets-high-power-supplies.

17. Valentine, N., Azarian, M.H., & Pecht, M. (2019). Metallized film capacitors used for EMI filtering: a reliability review. *Microelectronics Reliability* vol. 92 pp. 123–135.

18. Davis, J. L., Mills, K., Yaga, R., Johnson, C., & Young, J. (2017). Assessing the reliability of electrical drivers used in LED-based lighting devices. In W. D. van Driel, X. Fan, & G. Q. Zhang (Eds.), *Solid state lighting reliability part 2: Components to systems*. Springer.

19. Next Generation Lighting Industry Alliance, LED Systems Reliability Consortium. (2014). *LED luminaire lifetime: Recommendations for testing and reporting, Third Edition.* Washington, DC. Available from https://energy.gov/sites/prod/files/2015/01/f19/led_luminaire_lifetime_guide_sept2014.pdf.

20. Davis, J. L., & Mills, K. (2017). *System reliability model for solid-state lighting (SSL) luminaires. Final report of DOE project DE-EE0005124*. Washington, DC: U.S. Department of Energy.

21. Zhang, Y., Cai, Z., Suhling, J.C., Lall, P., & Bozack, M. (2009). The effects of SAC alloy composition on aging resistance and reliability. *2009 59th Electronic Components and Technology Conference (ECTC).* San Diego, CA. May 26-29, 2009. doi: 10.1109/ECTC.2009.5074043.

22. Teng, S., & Page, E. (2017). LED Lab Test Study: Final Report on 2013-2014 Work Order. Sacramento, CA: California Public Utilities Commission. Available from https://pda.energydataweb.com/api/view/1950/LED_Lab_Test_Report.pdf.

23. On Semiconductor. (2008). Transient Overvoltage Protection. Publication Order Number TND336/D. Available from http://www.onsemi.com/pub_link/Collateral/TND335-D.PDF.

24. Perrin, T. E., Brown, C. C., Poplawski, M. E., & Miller, N. J. *Characterizing photometric flicker. Report Number PNNL-25135.* Washington, D.C.: DOE, 2017. Available from https://energy.gov/sites/prod/files/2016/03/f30/characterizing-photometric-flicker.pdf.

25. Mehr, M.Y., Bahrami, A., van Driel, W.D., Fan, X.J., Davis, J. Lynn, & Zhang, G.Q. 2019. Degradation of optical materials in solid-state lighting systems. *International Materials Reviews*. doi: https://doi.org/10.1080/09506608.2019.1565716.

26. RTI International. (2013). *Hammer testing findings for solid-state lighting luminaires*. Prepared for the U.S. Department of Energy. Available from https://www1.eere.energy.gov/buildings/publications/pdfs/ssl/hammer-testing_Dec2013.pdf.

U.S. DEPARTMENT OF
ENERGY

Office of
**ENERGY EFFICIENCY &
RENEWABLE ENERGY**